

Chapter 1

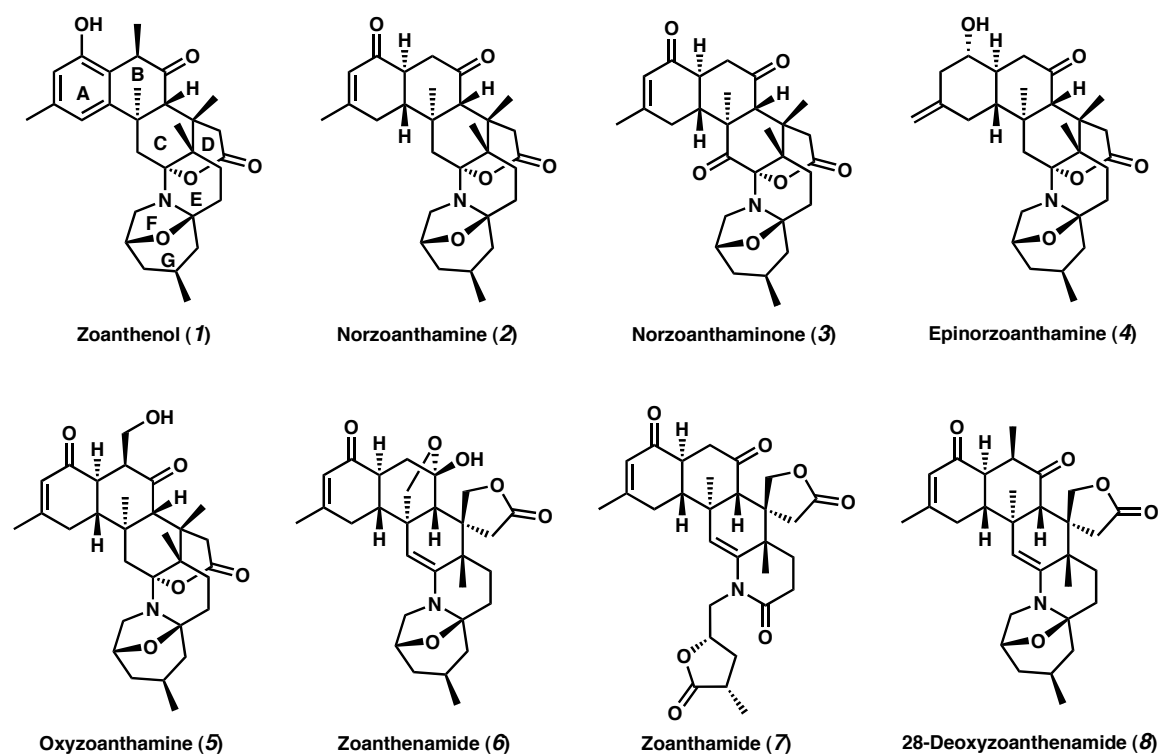
Progress Toward the Total Synthesis of Zoanthenol

I. Introduction

Zoanthid Natural Products

Zoanthenol **1** (Figure 1) is a member of the zoanthamine family of natural products, isolated from marine polyps (*Zoanthus sp.*) in 1999 off of the coast of India.¹ While zoanthenol **1** is a selective inhibitor of collagen-induced human platelet aggregation,² the range of zoanthus alkaloids exhibit interesting biological activities.

Figure 1. Zoanthamine natural products

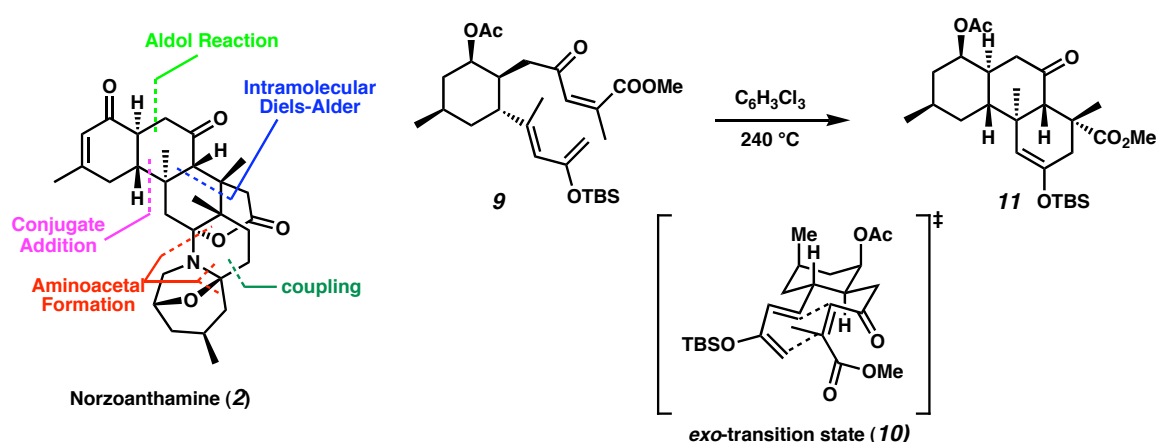


For example, norzoanthamine **2**, norzoanthaminone **3**, epinorzoanthamine **4**, and oxyzoanthamine **5** are all P388 murine leukemia inhibitors. Norzoanthamine **2** is also a potent antiosteoporotic due to its inhibitory activity against interleukin-6, and has been shown to counteract decreases in bone weight and strength in ovariectomized mice.³ Additionally, zoanthenamide **6**, zoanthamide **7**, and 28-deoxyzoanthenamide **8** all inhibit inflammation induced by phorbol myristate acetate (PMA) in a mouse-ear model.

Background

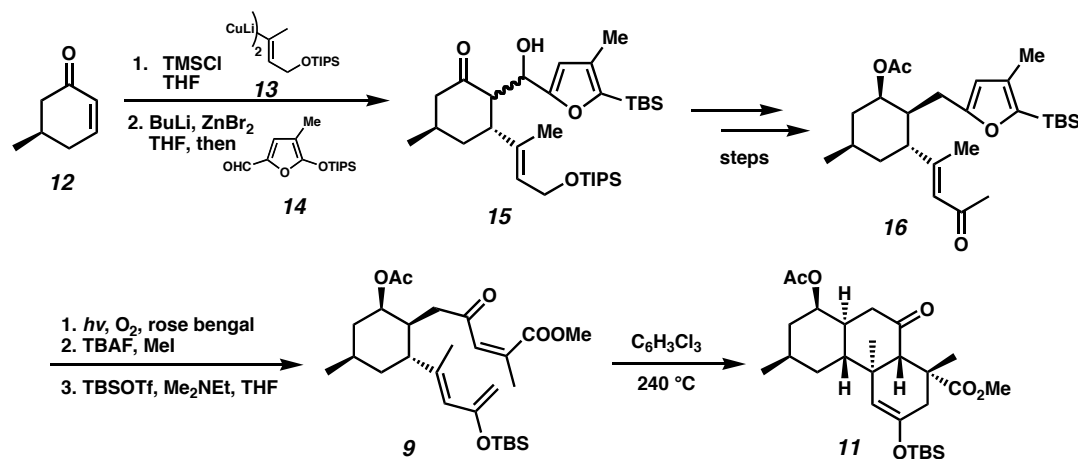
Despite the large structural diversity of the zoanthus alkaloids, the fact that several years have passed since their structural elucidation, and a number of relevant synthetic studies have been published, only a single total synthesis of a zoanthus alkaloid has been reported to date.⁴ The total synthesis of norzoanthamine was completed in 2004 by Miyashita and coworkers. As shown in Scheme 1, they dissected the structure of norzoanthamine **2** by a number of bond disconnections, with the key step in their synthesis resting on the formation of the ABC ring system.

Scheme 1. Miyashita's intramolecular Diels-Alder reaction



They constructed the tricycle with an intramolecular Diels-Alder reaction of triene **9**, which proceeded *via* *exo*-transition state **10** to form **11** as a mixture of cycloadducts in 98% combined yield. The intramolecular Diels-Alder substrate **9** was synthesized in 14 steps from the known chiral enone **12** by sequential C–C bond forming reactions including a diastereoselective cuprate addition with cuprate **13** and an aldol reaction with aldehyde **14** (Scheme 2), to provide furanol **15**. After elaboration of **15** to enone **16**, the tethered diene/dienophile pair are unveiled after functional group manipulation to provide Diels-Alder substrate **9**.

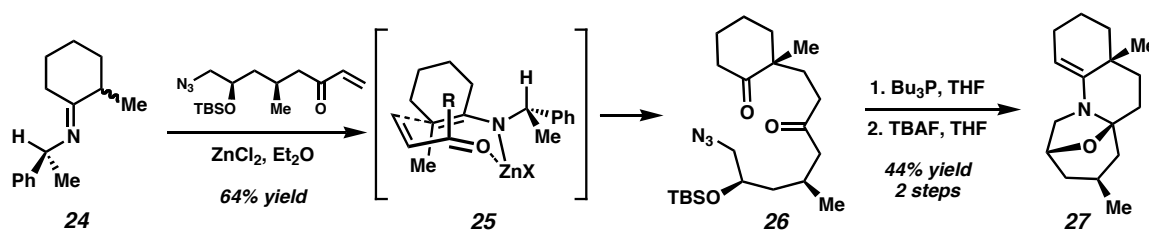
Scheme 2. Synthesis of the Diels-Alder substrate



After the Diels-Alder reaction, tricycle **11** is further elaborated into alkyne **17** in 14 synthetic steps (Scheme 3). Fragment coupling between alkyne **17** and an aldehyde occurs by nucleophilic attack to provide yne-one **18** after oxidation. Following reduction of the yne-one, the acetonide is selectively removed upon exposure to mild acid, and the system cyclizes to form hemi-aminal **19**, which is converted into triketone **20** in several steps. At this stage, the final aminal cyclization event is triggered by strongly acidic conditions and the final product is free-based to provide norzoanthamine **2**.

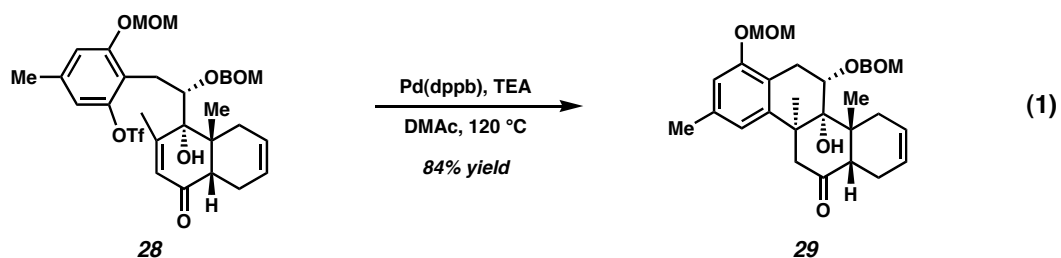
Williams also published an approach to the CEFG ring system of zoanthid alkaloids involving a diastereoselective conjugate addition directed by the chiral enamine **24**, which may proceed through contact pair **25** (Scheme 5). A minimization of non-bonding allylic interactions of the chiral controller unit present in transition state **25** dictates the facial approach of the enone opposite to the phenyl group.

Scheme 5. Williams' tandem amination cyclization

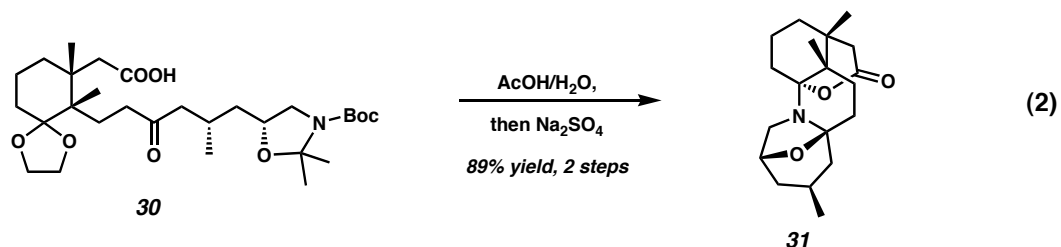


While transition structure **25** rationalizes the stereochemical outcome of the metallo-enamine reaction, reactions of this type may progress through an aza-ene mechanism with concerted proton transfer, or *via* formation of a hetero-Diels-Alder dihydropyran with subsequent isomerization.⁶ In either event, the Michael adduct **26** was obtained in good yield and diastereoselectivity. Subsequently, a tandem Staudinger reaction/intramolecular aza-Wittig condensation provided **27** after desilylation.⁷

In other synthetic studies aimed at zoanthid natural products, Hirama and coworkers demonstrate progress toward zoanthenol **1** using an intramolecular Heck reaction of aryl triflate **28** to close the B-ring with high diastereoselectivity to provide **29** in good yield (eq 1).⁸



Finally, Kobayashi has completed a diastereoselective synthesis of the CDEFG-ring system **31** in good yield by demonstrating the biogenic acid-catalyzed tandem aminal cyclization on protected amino-alcohol **30** (eq 2).⁹



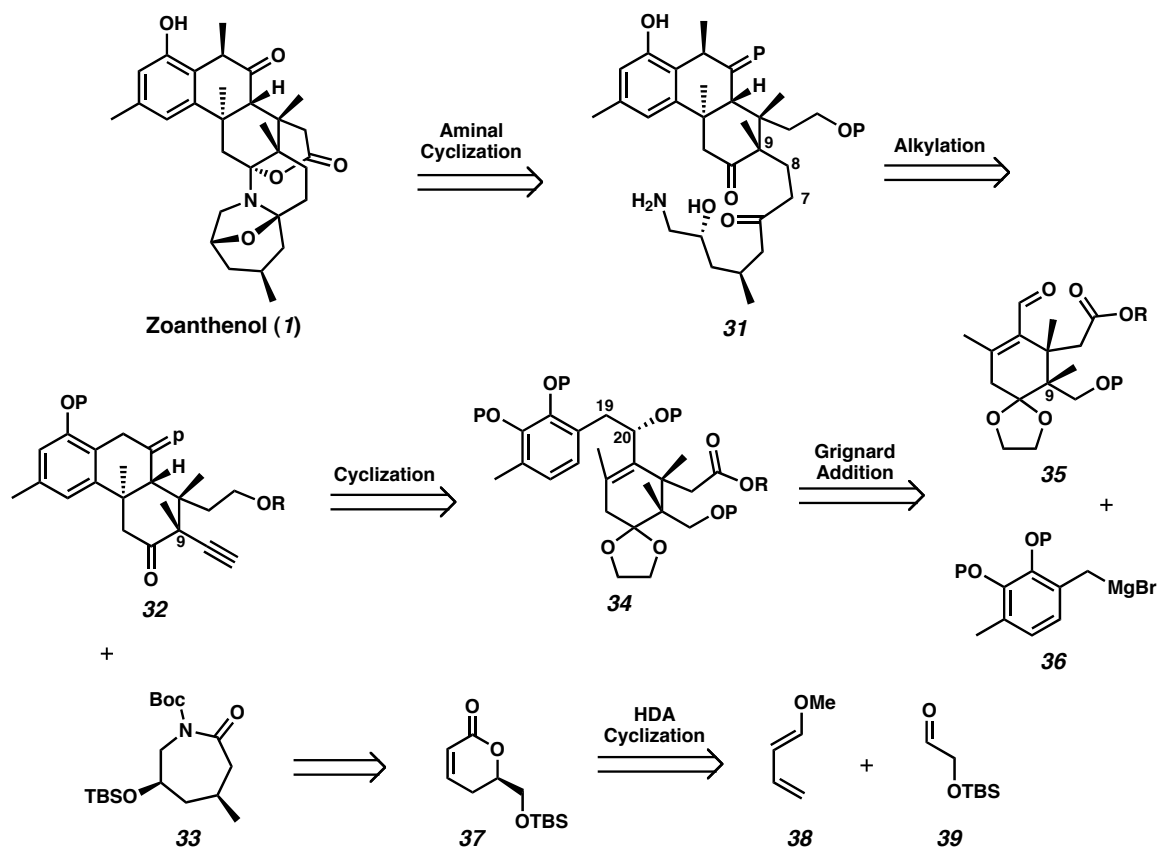
While there are a number of published synthetic studies towards zoanthid natural products, they remain formidable targets for total synthesis, as only norzoanthamine **2** has been synthesized. Intrigued by its structural complexity, we initiated synthetic studies towards the enantioselective total synthesis of zoanthenol **1**.

Retrosynthetic Analysis

Zoanthenol presents a stimulating challenge for total synthesis owing to its intricate array of nine stereocenters, including three quaternary stereocenters, and complex polycyclic architecture. Furthermore, the heteroatom distribution in the lower four rings constitutes an unusual bis-aminal ring system. The complex structure of zoanthenol **1** allows for late stage disconnection of the aminal moiety (Figure 2), immediately reducing the heptacyclic natural product to a tricyclic system appended with a linear fragment as

shown in structure **31**. Another C–C bond disconnection reduces **31** into tricycle **32** and caprolactam **33**. Fragment **32** may be disconnected to provide the cyclization substrate **34**, which is constructed from aldehyde **35** and Grignard **36**.

Figure 2. Retrosynthetic analysis of zoanthenol

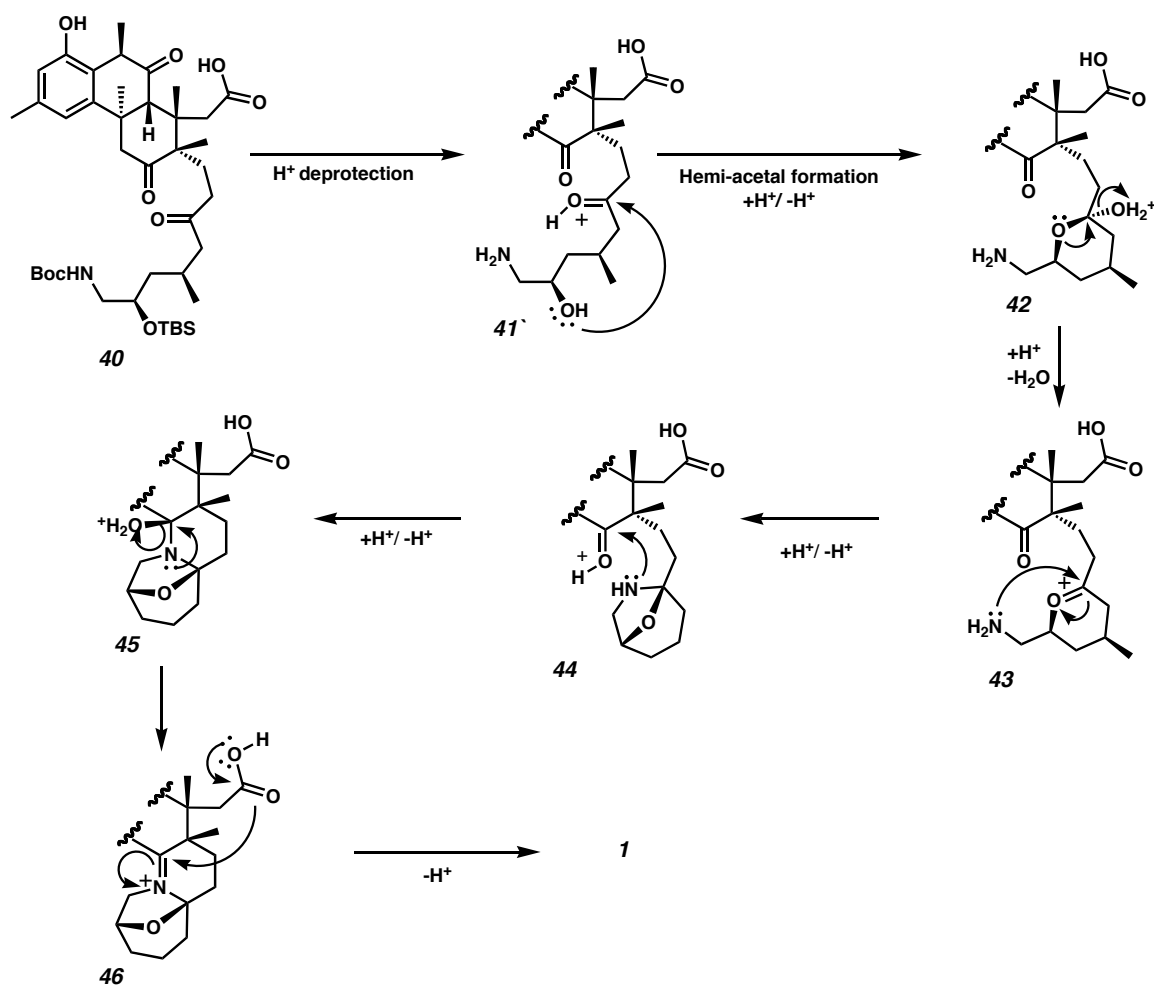


Synthetic studies on tricycle **32** are currently under pursuit by graduate students Doug Behenna and Jennifer Stockdill, and will not be detailed here. Instead, this discussion will focus on the synthesis of caprolactam **33**, which is accessible through the unsaturated lactone **37**. Intermediate **37** is in turn generated directly from diene **38** and aldehyde **39** by an enantioselective hetero-Diels-Alder reaction.

Mechanistic Considerations of the Tandem Aminal Cyclization

The disconnection from zoanthenol **1** to amino alcohol **31** (Figure 2) suggests the biogenesis of zoanthenol.¹ The fully constructed aminal ring system likely represents one end of an intricate equilibrium. A plausible mechanism for the proposed synthetic cyclization event, shown in Figure 3, is based on the assumptions that 1) full deprotection occurs before any bond forming event and that 2) five- and six-membered ring acetal formation is much faster than any higher membered ring.

Figure 3. A reasonable mechanism for the cyclization



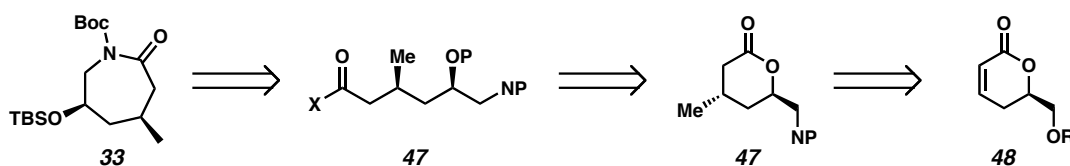
Under acidic conditions, full deprotection of advanced carbocycle **40** results in amino alcohol **41**, which is likely to form the kinetically favored six-membered hemi-acetal **42**. After protonation of the hemi-acetal, donation of the lone pair from the newly formed ether produces oxo-carbenium ion **43**. The oxo-carbenium ion is suitably disposed for attack by the nearby nitrogen lone pair to close the bicyclic aminal **44**. After proton shift, the resulting aminal **45** may now close as a six-membered ring, forming iminium ion **46**. The iminium ion is subsequently quenched upon nucleophilic attack of the nearby carbonyl, closing the final six-membered ring to provide zoanthenol (**1**).

II. Results and Discussion

Retrosynthetic analysis of the DEFG ring precursor

Early on, we identified caprolactam **33** as an essential fragment in the total synthesis of zoanthenol (Figure 4). Simple disconnection across the amide functionality provides the protected linear amino-alcohol **47**, which may be constructed from a six-membered lactone **47**, a more common structural subunit than the seven-membered lactam **33**. Further retrosynthetic removal of a methyl equivalent from lactone **47** provides the known α,β -unsaturated δ -lactone **48**.¹⁰

Figure 4. Retrosynthesis of caprolactam **33**



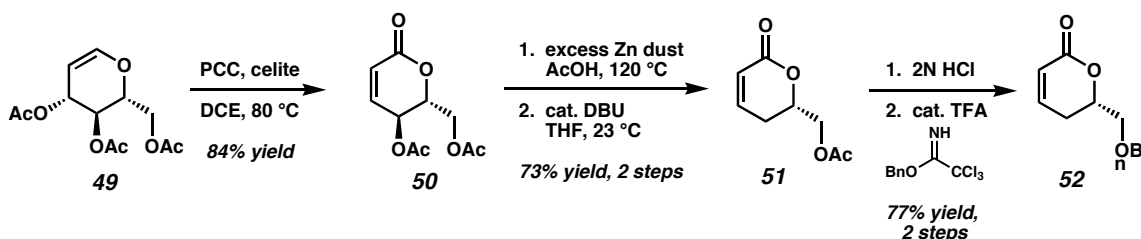
With a clearly defined set of goals (i.e., synthesis of caprolactam **33** via a δ -lactone of type **48**), we began synthetic efforts to determine a fast and efficient enantioselective synthesis of this major natural product fragment present in many of the zoanthid natural products, including zoanthenol **1**.

Synthetic Route from the Chiral Pool

Our first efforts focused on utilizing the chiral pool as a starting point for the synthesis of an α,β -unsaturated lactone of type **48**. Literature preparations detail the synthesis of several intermediates *en route* to lactone **48** from tri-O-acetyl-*D*-glucal **49**.¹¹ While both enantiomers of the required sugar are commercially available, tri-O-acetyl-*D*-glucal **49** is much cheaper than the (*L*)-enantiomer, which is ultimately required for the synthesis of zoanthid natural products according to our synthetic plan. To minimize the cost of materials, initial synthetic investigation was conducted on the inexpensive (*D*)-glucal.

Starting from tri-O-acetyl-*D*-glucal **49**, unsaturated lactone **50** was accessed in good yield by PCC oxidation according to known methods (Scheme 6).¹² The extraneous acetate was removed by reductive deconjugation with activated Zn dust in acetic acid, providing lactone **51**, upon re-conjugation by treatment with catalytic DBU.¹² Following removal of the acetate group, our initial attempts at protection with a more suitable group were unproductive because intermediates related to **51** were very sensitive to base, and the route was abandoned in favor of another approach (see Scheme 7). Ultimately, mild acidic conditions for the benzyl protection were developed, providing δ -lactone **52**, which was identical to material produced by published methods.¹³

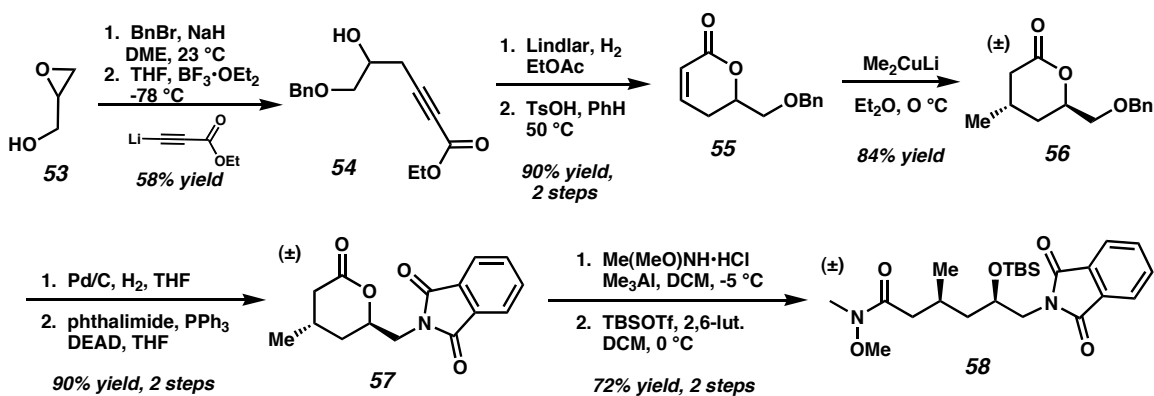
Scheme 6. Sugar route



Synthetic Route from Glycidol

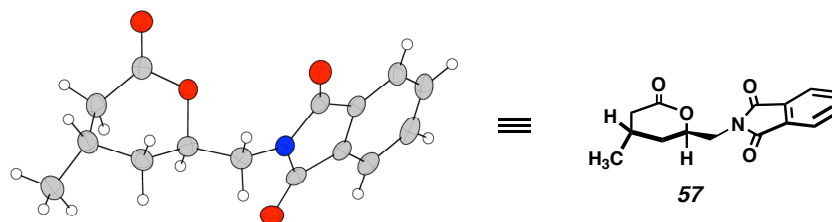
Despite the initial appeal of utilizing the chiral pool as the starting point for the synthesis of enone **52**, both the necessity to alter protecting groups, and the initial difficulty in doing so, prompted the exploration of a route starting from racemic glycidol **53**. The enantioselective route could be secured upon completion of the racemic route from readily available (*S*)-glycidol.^{14,15} According to literature preparations, the sequence began with benzyl protection of racemic glycidol **53**, followed by nucleophilic epoxide opening with the anion of ethyl propiolate to provide the known alkyne **54** (Scheme 7).¹⁶

Scheme 7. Synthetic route from glycidol



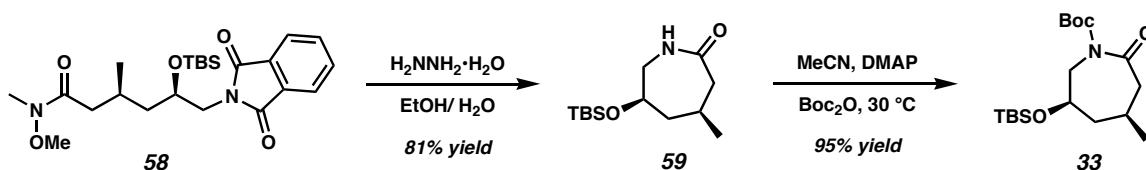
Unsaturated lactone **55** was quickly accessed through Lindlar reduction of alkyne **54**, followed by cyclization upon exposure to mild acid. With the suitably protected lactone **55** in hand, a highly diastereoselective cuprate addition with the Gilman reagent proceeded smoothly, yielding scaleable quantities of the saturated lactone **56** as a single observed diastereomer. Installation of the primary amine was accomplished through hydrogenolysis of the benzyl ether, followed by a Mitsunobu reaction with phthalimide, providing the crystalline intermediate **57**. X-ray analysis of **57** confirms the relative stereochemistry resulting from the cuprate addition (Figure 5).

Figure 5. X-ray structure of phthalimide adduct **57**



The Weinreb amide **58** was prepared from lactone **57** and the intermediate alcohol was immediately trapped as the TBS ether to prevent the facile closure to starting material, generating amide **58** (Scheme 7). Decomposition of the phthalimide moiety present in **58** with hydrazine hydrate in refluxing ethanol released the latent amine functionality, which immediately cyclized to provide caprolactam **59** (Scheme 8). Protection of the amide as the *t*-butylcarbamate provided **33**, a key retron for the total synthesis of **1**.

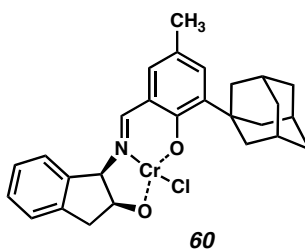
Scheme 8. Advancing to the final retron



Synthesis of key lactone via a hetero-Diels Alder cyclization.

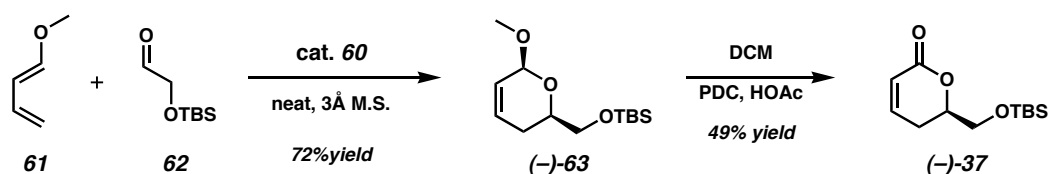
Despite having developed a reaction sequence readily applicable to enantioselective synthesis, our attentions were soon drawn to a more direct route to an equivalent of key lactone **52**. Jacobsen et al. have demonstrated that the chromium complex **60** is an effective catalyst for enantioselective hetero-Diels-Alder (HDA) reactions between aldehydes and electron rich dienes.⁶

Figure 6. Jacobsen hetero-Diels-Alder catalyst



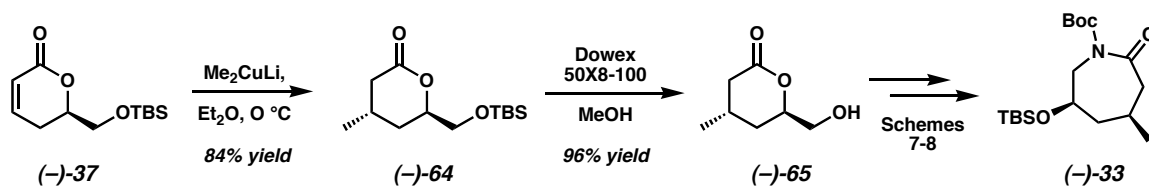
According to their method,¹⁷ simply by combining the diene **61**, the aldehyde **62**, and a catalytic quantity of chromium catalyst **60**, we observed the highly diastereo- and enantioselective synthesis of glycol (–)-**63** in 72% yield and >99% ee. Subsequent PDC oxidation of glycol (–)-**63** in the presence of wet acetic acid provided enone (–)-**37** (Scheme 9).

Scheme 9. Enantioselective hetero-Diels-Alder reaction



Conjugate addition with the Gilman reagent into unsaturated lactone **(-)-37** provided the *anti*-disubstituted lactone **(-)-64** as a single observed diastereomer (Scheme 10). Mild desilylation in the presence of a resin-bound acid source provided the unprotected alcohol **(-)-65**, which was elaborated to the caprolactam **(-)-33** as previously described (Schemes 7-8). All intermediates in the enantioselective route were analytically identical to those in the racemic route by ^1H NMR and ^{13}C NMR analysis.

Scheme 10. Advancing enantiopure synthetic intermediates

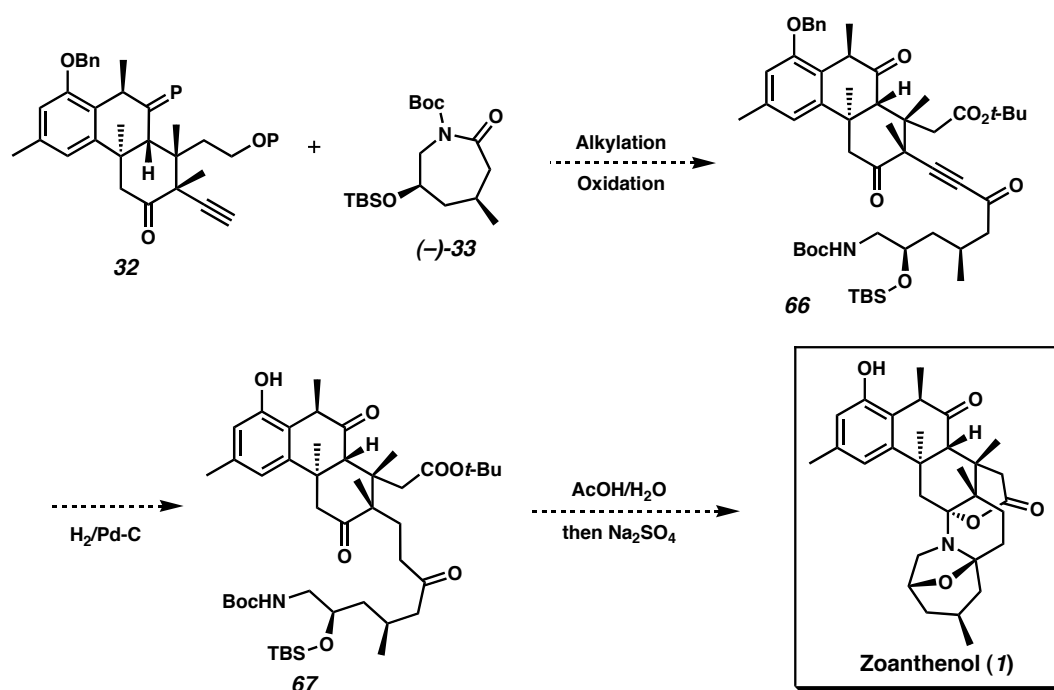


Endgame for the Total Synthesis of Zoanthenol

Upon completion of the ABC ring **32**, fragment coupling with caprolactam **(-)-33** will provide yne-one **66** after oxidation (Scheme 11).¹⁸ After deprotection and further oxidation, hydrogenolysis of both the alkyne and the benzyl ether present in **66** is expected to generate the advanced intermediate **67**. Treatment with acid is expected to

initiate the ultimate tandem aminal cyclization, completing the total synthesis of zoanthenol **1**.

Scheme 11. Endgame for zoanthenol



III. Conclusion

With the goal of establishing a synthetic route to enantiopure caprolactam (-)-**33**, three routes to the key δ -lactone of type **44** were explored. Our initial plan to derive the desired lactone from the chiral pool was soon abandoned due to preliminary synthetic difficulties. A more modern method utilizing glycidol as the starting material was explored, resulting in successful delivery of the racemic caprolactam **33**. Ultimately, enantiopure δ -lactone (-)-**37** was obtained by means of a highly diastereoselective and

enantioselective hetero-Diels-Alder cyclization. Key features of the subsequent synthesis include a highly diastereoselective cuprate addition and a protecting group strategy for the masking of the reactive amino alcohol moiety. The enantiopure caprolactam (–)-**33** generated by the detailed method is expected to be a competent electrophile for coupling with the appropriate nucleophile of alkynyl-tricycle **32**. After fragment coupling, only a few synthetic transformations are expected to complete the total synthesis of zoanthenol **1**.

IV. Experimental Section

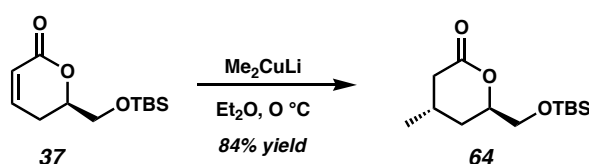
Materials and Methods

Unless stated otherwise, reactions were conducted in flame-dried glassware using anhydrous solvents (either freshly distilled or passed through activated alumina columns). All reactions were conducted under an inert atmosphere of dry nitrogen or argon, unless otherwise stated. All commercially obtained reagents were used as received. When required, commercial reagents were purified following the guidelines of Perrin and Armarego.¹⁹ Reaction temperatures were controlled using an IKAmag temperature modulator. Thin-layer chromatography (TLC) was conducted with E. Merck silica gel 60 F254 pre-coated plates (0.25 mm) and visualized using a combination of UV, anisaldehyde, ceric ammonium molybdate, and potassium permanganate staining. ICN silica gel (particle size 0.032–0.063 mm) was used for flash chromatography using the method described by Still.²⁰

¹H NMR spectra were recorded on a Varian Mercury 300 (at 300 MHz), a Varian Inova 500 (at 500 MHz), and are reported relative to residual protio solvent signals. Data for ¹H NMR spectra are reported as follows: chemical shift (δ ppm), multiplicity (s = singlet, d = doublet, t = triplet, q = quartet, m = multiplet), coupling constant (Hz), and integration. ¹³C NMR spectra were recorded on a Varian Mercury 300 (at 75 MHz) and are reported relative to residual protio solvent signals. Data for ¹³C NMR spectra are reported in terms of chemical shift. IR spectra were recorded on a Perkin Elmer Paragon 1000 spectrometer and are reported in frequency of absorption (cm^{-1}). Optical rotations were measured with a Jasco P-1010 polarimeter (Na lamp, 589 nm). HPLC analysis was performed on a Hewlett-Packard 1100 Series HPLC (UV detector at 245 nm) equipped

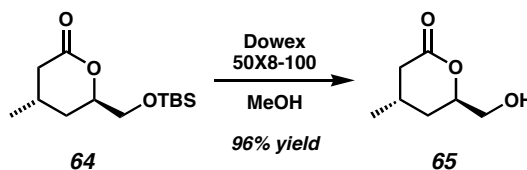
with the following Chiralcel columns: OD-H (25 cm), OD guard (5 cm), AD (25 cm), OJ (25 cm) and OB-H (25 cm). High resolution mass spectra were obtained from the California Institute of Technology Mass Spectral Facility.

Preparative Procedures

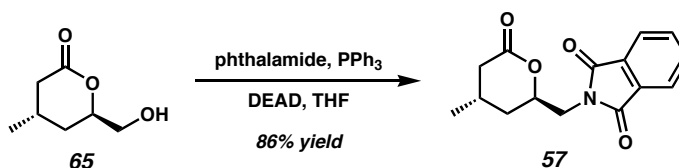


β -Me, δ -Lactone (64). MeLi (1.3 M in ether, 5.8 mL, 7.56 mmol) was added to a stirring slurry of CuI (714 mg, 3.89 mmol) in diethyl ether cooled to $-78\text{ }^\circ\text{C}$. The vessel was warmed to $0\text{ }^\circ\text{C}$ for 15 min, then cooled again to $-78\text{ }^\circ\text{C}$. A solution of the α,β -unsaturated lactone **37** (471 mg, 1.95 mmol) in diethyl ether (4 mL) was then carefully added along the cooled inner walls of the reaction flask. After 1 h, the reaction mixture was quenched by the slow addition of saturated aq ammonium chloride (15 mL) at $-78\text{ }^\circ\text{C}$. The reaction flask was gradually warmed to ambient temperature for 30 min, then diluted with ether (30 mL). The biphasic mixture was transferred to a separatory funnel and shaken vigorously to dissolve solids. The organic layer was washed with saturated aq ammonium chloride (2 x 20 mL), then brine (1 x 10 mL), dried over magnesium sulfate and concentrated. The resulting material was purified by flash chromatography over silica gel (25% EtOAc:hexane eluent) to yield δ -lactone **64** (422 mg, 84% yield, $R_f = 0.20$ in 25% EtOAc:hexane) as a clear oil: ^1H NMR (300 MHz, CDCl_3) δ 4.47-4.40 (m, 1H), 3.70-3.73 (m, 2H), 2.55 (dd, $J = 16.3, 5.1$ Hz, 1H), 2.18-2.29 (m, 1H), 2.12 (dd, $J = 16.4, 8.9$ Hz, 1H), 1.90-1.99 (m, 1H), 1.52-1.60 (m, 1H), 1.05 (d, $J = 6.6$ Hz, 3H), 0.87 (s, 9H), 0.06 (s, 6H); ^{13}C NMR (75 MHz, CDCl_3) δ 171.7, 77.8, 65.1, 38.1, 31.7, 26.2, 24.1, 21.4, 18.6,

5.00; IR (neat) 1743 cm^{-1} ; HRMS (FAB⁺) m/z calc'd for $[\text{C}_{13}\text{H}_{26}\text{O}_3\text{Si}]^+$: 201.0947, found 201.0950; $[\alpha]_{\text{D}}^{20}$ -25.027° (c=1, CDCl_3).

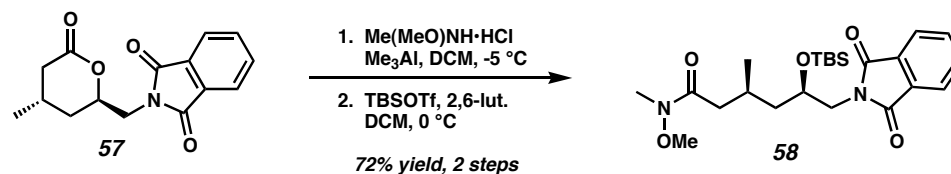


Alcohol 65. The lactone (100 mg, 0.39 mmol) was dissolved in methanol (5.0 mL) and added to a reaction flask equipped with Dowex 50X8-100 cation exchange resin (1.0 g). The mixture was stirred at ambient temperature for 3 h, then filtered. The resin was washed with methanol (2 x 5 mL) and the combined organics were concentrated. The crude material was dried overnight under high vacuum to yield the alcohol **65** (53 mg, 96% yield, R_{F} = 0.18 in 80% EtOAc:hexane) as a clear oil: ^1H NMR (300 MHz, CDCl_3) δ 4.47-4.52 (m, 1H), 3.75 (dd, J =12.3, 3.6 Hz, 1H), 3.66 (dd, J =12.1, 5.8 Hz, 1H), 2.69 (br s, 1H), 2.53-2.58 (m, 1H), 2.13-2.23 (m, 2H), 1.88-1.97 (m, 1H), 1.49-1.57 (m, 1H), 1.08 (d, J =6.0 Hz, 3H); ^{13}C NMR (75 MHz, CDCl_3) δ 172.3, 78.2, 65.1, 37.8, 31.1, 24.3, 21.4; IR (neat) 1722.4 cm^{-1} ; HRMS (FAB⁺) m/z calc'd for $[\text{C}_7\text{H}_{12}\text{O}_3]^+$: 144.0786, found 144.0787; $[\alpha]_{\text{D}}^{20}$ -162.147° (c=1, CDCl_3).



Phthalimide (57). To a stirred solution of alcohol **65** (1.48 g, 10.28 mmol) in tetrahydrofuran (30 mL) was added triphenyl phosphine (2.83 g 10.79 mmol), then

phthalimide (1.59 g, 10.76 mmol). Once all reagents had dissolved, the reaction mixture was cooled to 0 °C and DEAD (1.707 mL, 10.79 mmol) was added dropwise to the stirred solution. The reaction flask was then warmed to 30 °C for 12 h, then concentrated. The concentrated reaction mixture was flashed over silica (4:1 hexanes/EtOAc eluent). The resulting solid was recrystallized from dichloromethane to provide phthalimide **57** (2.42 g, 86% yield, R_F = 0.16 in 40% EtOAc:hexane) as a white solid: m.p. 118-120 °C; ^1H NMR (300 MHz, CDCl_3) δ 7.82-7.88 (m, 2H), 7.71-7.76 (m, 2H), 4.74-4.83 (m, 1H), 4.04 (dd, J =15.0, 8.3 Hz, 1H), 3.78 (dd, J =15.0, 5.5 Hz, 1H), 2.63 (dd, J =16.6, 5.4 Hz, 1H), 2.28 (m, 1H), 2.16 (dd, J =16.5, 9.1 Hz, 1H), 1.86 (m, 1H), 1.66 (m, 1H), 1.09 (d, J =6.9 Hz, 3H); ^{13}C NMR (300 MHz, CDCl_3) δ 170.9, 168.1, 134.4, 132.0, 123.7, 74.1, 41.9, 37.9, 32.8, 24.0, 21.5; IR (neat) 1773.9, 1715.8 cm^{-1} ; HRMS (FAB $^+$) m/z calc'd for $[\text{C}_{15}\text{H}_{16}\text{NO}_4]^+$: 274.1079, found 274.1076; $[\alpha]_D^{20}$ -68.6255° (c =1, CDCl_3).

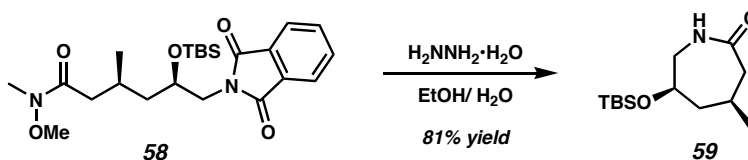


Weinreb Amide (58). Trimethylaluminum (2.0 M in toluene, 10.32 mL, 20.64 mmol) was slowly added to a stirred solution of *N,O*-dimethylhydroxylamine hydrochloride (2.01 g, 16.80 mmol) in dichloromethane (40 mL) cooled to $-10\text{ }^\circ\text{C}$. The solution was stirred for 20 min before the dropwise addition of the Mitsunobu adduct **57** (2.26 g, 8.23 mmol) in dichloromethane (10 mL). The reaction temperature was maintained at $-10\text{ }^\circ\text{C}$ for 30 min before the addition of saturated sodium bicarbonate (20

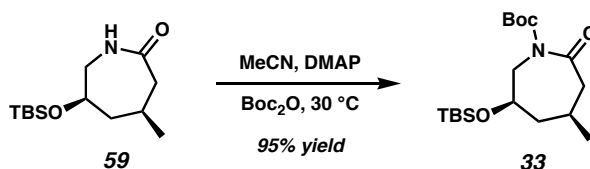
mL). The reaction mixture was then allowed to warm to room temperature. The crude reaction mixture was diluted with dichloromethane (30 mL) and brine (20 mL) to dissipate emulsions during extraction. The crude was transferred to a separatory funnel and the organic layer was separated. The aqueous layer was extracted with dichloromethane (2 x 30 mL). The combined organic layers were washed with brine (1 x 30 mL), then dried and concentrated to a volume of 10 mL over a rotovap pot temperature of 15 °C.

The crude amide was diluted with dichloromethane (20 mL) and cooled to 0 °C. To the cooled, stirred solution was added TBSOTf (3.79 mL, 16.51 mmol) followed by 2,6-lutidine (1.442 mL, 12.38 mmol). The solution was maintained at 0 °C for 20 min, then quenched by addition of saturated ammonium chloride (20 mL). The biphasic mixture was allowed to warm to room temperature while stirring vigorously, then transferred to a separatory funnel. The organic layer was separated and the aqueous layer was extracted with dichloromethane (2 x 20 mL). The combined organics were washed with saturated sodium bicarbonate solution (1 x 15 mL) and water (1 x 15 mL), then dried over magnesium sulfate and concentrated. The resulting crude product was flashed over silica gel (20% EtOAc:hexanes eluent) to provide Weinreb amide **58** (2.58g, 72% yield, R_F = 0.30 in 40% EtOAc:hexane) as an oil: ^1H NMR (300 MHz, CDCl_3) δ 7.82 (dd, J =5.4, 3.1 Hz, 2H), 7.70 (dd, J =5.6, 2.9 Hz, 2H), 4.05-4.14 (m, 1H), 3.68-3.78 (m, 2H), 3.65 (s, 3H), 3.14 (s, 3H), 2.38-2.45 (m, 1H), 2.18-2.29 (m, 1H), 1.51-1.60 (m, 1H), 1.38-1.47 (m, 1H), 1.03 (d, J =6.3 Hz, 3H), 0.76 (s, 9H), -0.01 (s, 3H), -0.20 (s, 3H); ^{13}C NMR (300 MHz, CDCl_3) δ 168.5, 134.1, 132.3, 123.3, 68.3, 61.5, 44.0, 43.7, 39.7, 32.3, 26.9, 26.0, 20.8, 18.1, -4.3, -4.4; IR (neat) 3473.5, 2955.4, 2857.3, 1774.2, 1714.5, 1660.3

cm⁻¹; HRMS *m/z* calc'd for [C₂₃H₃₇N₂O₅Si]⁺: 449.2472, found 449.2470; [α]_D²⁰ -29.7° (c=1, CDCl₃).



Caprolactam 59. To a solution of **58** (2.848 g, 6.55 mmol) in absolute ethanol was added hydrazine monohydrate (1.75 mL, 32.77 mmol) and deionized water (0.39 mL). The solution was heated to 90 °C for 4 h. The reaction was then cooled in an ice bath and the thick cottony solids were filtered. The filtrate was then concentrated to a solid. The crude solid was taken up in EtOAc (50 mL), cooled in an ice bath, and filtered over a pad of Celite, rinsing with portions of EtOAc (2 x 20 mL). The organics were then dried over sodium sulfate and concentrated. The crude solid was subjected to chromatography over silica gel (30% EtOAc:hexane eluent) to yield the unprotected caprolactam **59** (1.633g, 81% yield, R_F= 0.22 in 50% EtOAc:hexane) as a white solid: m.p. 79-81 °C; ¹H NMR (300 MHz, CDCl₃) δ 6.27 (br s, 1H), 3.56-3.65 (m, 1H), 3.18-3.28 (m, 1H), 3.01-3.10 (m, 1H), 2.38 (dd, *J*=13.7, 11.0 Hz, 1H), 2.25 (dd, *J*=12.1, 1.7 Hz, 1H), 1.96-2.04 (m, 1H), 1.83-1.93 (m, 1H), 1.36 (q, *J*=11.8 Hz, 1H), 1.04 (d, *J*=6.9 Hz, 3H), 0.86 (s, 9H), 0.05 (s, 6H); ¹³C NMR (300 MHz, CDCl₃) δ 177.3, 71.0, 49.7, 48.9, 44.2, 28.6, 26.1, 24.8, 18.4, -4.2, -4.4; IR (neat) 3239.9, 2929.8, 2857.6, 1673.1 cm⁻¹; HRMS (EI⁺) *m/z* calc'd for [C₁₃H₂₈NO₂Si]⁺: 242.1576, found 242.1576; [α]_D²⁰ -15.0° (c=1, CDCl₃).

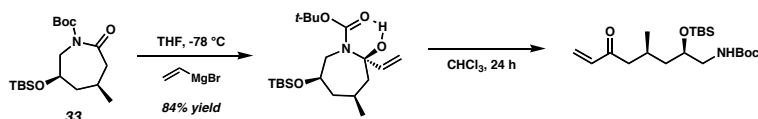


***N*-Boc-caprolactam (33).** To a solution of **33** (853 mg, 3.313 mmol) in acetonitrile (40 ml) was added *t*-butyl carbonate anhydride (1.81 g, 8.28 mmol). After the *t*-butyl carbonate anhydride had completely dissolved, *N,N*-dimethylamino pyridine (1.01 g, 8.28 mmol) was added in several small portions. The resulting dark-brown solution was stirred for 10 min at ambient temperature, then warmed to 35 °C. After 5 hours, the reaction was quenched by addition of water (20 mL). The mixture was transferred to a separatory funnel and extracted with EtOAc (4 x 30 mL). The combined organics were washed with brine (1 x 30 mL), dried over sodium sulfate, and concentrated to give a brown waxy solid, which was purified by flash chromatography over silica (10% EtOAc:hexane) to provide *N*-Boc-caprolactam **33** (1.314 g, 95% yield, $R_F = 0.22$ in 10% EtOAc:hexane) as a waxy solid: m.p. 77-78°; ^1H NMR (300 MHz, CDCl_3) δ 4.11 (dt, $J=14.8, 1.8$ Hz, 1H), 3.63 (tdd, $J=22.0, 4.9, 2.2$ Hz, 1H), 3.33 (dd, $J=15.0, 9.5$ Hz, 1H), 2.56 (dd, $J=14.1, 10.9$ Hz, 1H), 2.41 (d, $J=14.3$ Hz, 1H), 1.96-2.03 (m, 1H), 1.87-1.94 (m, 1H), 1.51 (s, 9H), 1.27-1.39 (m, 1H), 1.04 (d, $J=6.6$ Hz, 3H), 0.87 (s, 9H), 0.09 (s, 3H), 0.07 (s, 3H); ^{13}C NMR (300 MHz, CDCl_3) δ 174.1, 152.5, 83.4, 70.4, 52.4, 47.7, 47.0, 28.4, 28.1, 26.1, 24.5, 18.4, 4.3, 4.4; IR (neat) 2932.4, 1710.2, 1645.1 cm^{-1} ; HRMS m/z calc'd for $[\text{C}_{18}\text{H}_{36}\text{NO}_4\text{Si}]^+$: 358.2414, found 358.2426; $[\alpha]_D^{20}$ -48.0° ($c=1$, CDCl_3).

IV. Notes and References

- (1) (a) Rao, C.B.; Anjaneyula, A.S.; Sarma, N.S.; Venkatateswarlu, Y.; Rosser, R.M.; Faulkner, D. J.; Chen, M. H.; Clardy J. *J. Am. Chem. Soc.* **1984**, *106*, 7983. (b) Rao, C. B.; Anjaneyula, A. S.; Sarma, N. S.; Venkatateswarlu, Y.; Rosser, R. M.; Faulkner, D. J. *J. Org. Chem.* **1985**, *50*, 3757. (c) Rao, C.B.; Rao, D.V.; Raju, V.S.; Raju, B.W.; Sullivan, B.W.; Faulkner, D.J. *Heterocycles* **1989**, *28*, 103. (d) Fukuzawa, S.; Hayashi, Y.; Uemura, D.; Nagatsu, A.; Yamada, K.; Ijyuin, Y. *Heterocycl. Commun.* **1995**, *1*, 207.
- (2) Villar, R. M.; Gil-Longo, J.; Daranas, A. H.; Souto, M. L.; Fernández, J. J.; Peixinho, S.; Barral, M. A.; Santafé, G.; Rodríguez, J.; Jiménez, C. *Bioorg. Med. Chem.* **2003**, *11*, 2301.
- (3) Kuramoto, M.; Hiyashi, K.; Fujitani, Y.; Yamaguchi, K.; Tsuji, T.; Yamada, K.; Ijuin, Y.; Uemura, D. *Tetrahedron Lett.* **1997**, *38*, 5683.
- (4) Miyashita, M.; Sasaki, M.; Hattori, I.; Sakai, M.; Tanino, K., *Science* **2004**, *305*, 495.
- (5) Williams, D. R.; Brugel, T. A. *Org. Lett.* **2000**, *2*, 1023.
- (6) Hickmott, P.W. *The Chemistry of Enamines, Part 1* John Wiley & Sons, Inc.: New York, 1994, 843-871.
- (7) Williams, D. R.; Cortez, G. S. *Tetrahedron Lett.* **1998**, *39*, 2675.
- (8) Hirai, G.; Koizumi, Y.; Moharram, S. M.; Oguri, H.; HIRAMA, M. *Org. Lett.* **2002**, *4*, 1627.
- (9) Hikage, N.; Furukawa, H.; Takao, K.; Kobayashi, S. *Chem. Pharm. Bull.* **2000**, *48*, 1370.
- (10) The lactone is a common synthetic intermediate used in the synthesis of several natural products, including compactin and mevinoline. For references, see: (a) Bauer, T.; Chapuis, C.; Jezewski, A.; Kozak, J.; Jurczak, J. *Tetrahedron: Asymm.* **1996**, *7*, 1391. (b) Cardani, S.; Scolastico, C.; Villa, R. *Tetrahedron* **1990**, *46*, 7283. (c) Bauer, T.; Kozak, J.; Chapuis, C.; Jurczak, J. *J. Chem. Soc., Chem. Commun.* **1990**, *17*, 1178.
- (11) (a) Roth, B. D.; Roark, W. H. *Tetrahedron Lett.* **1988**, *29*, 1255. (b) Lichtenhaler, F. W.; Lorenz, K.; Ma, W. *Tetrahedron Lett.* **1987**, *28*, 47. (c) Rollin, P.; Sinay, P. *Carbohydrate Res.* **1981**, *98*, 139.

- (12) Roth, B. D.; Roark, H. *Tetrahedron Lett.* **1988**, *29*, 1255.
- (13) Synthesized from a Diels-Alder reaction using a chiral controller, see: Bauer, T.; Chapuis, C.; Jezewski, A.; Kozak, J.; Jurczak, J. *Tetrahedron: Asymm.* **1996**, *7*, 1391.
- (14) (a) Takano, S.; Shimazaki, Y.; Moriya, M.; Ogasawara, K. *Chem. Lett.* **1990**, 1177. (b) Takano, S.; Shimazaki, Y.; Iwabuchi, Y.; Ogasawara, K. *Tetrahedron Lett.* **1990**, *31*, 3619.
- (15) Furrow, M.E.; Schaus, S. E.; Jacobsen, E. N. *J. Org. Chem.* **1998**, *63*, 6776-6777.
- (16) Prepared according to the procedure given by: Oizumi, M.; Takahashi, M.; Ogasawara, K. *Syn. Lett.* **1997**, *9*, 1111.
- (17) Dossetter, A. G.; Jamison, T. F.; Jacobsen, E. N. *Angew. Chem. Int. Ed.* **1999**, *38*, 2398-2400.
- (18) Caprolactam **33** is expected to be an excellent coupling partner for a single electrophilic addition, without competing double anion addition. In a test reaction (see below) with excess vinyl magnesium bromide, the tetrahedral intermediate was an isolable intermediate, which collapsed to the linear species upon standing.



- (19) Perrin, D. D.; Armarego, W. L. F. *Purification of Laboratory Chemicals*; 3rd ed., Pergamon Press, Oxford, 1988.
- (20) Still, W. C.; Kahn, M.; Mitra, A. J. *J. Org. Chem.* **1978**, *43*, 2923.

APPENDIX ONE

Spectra Relevant to Chapter 1: Progress Toward the Total Synthesis of Zoanthenol

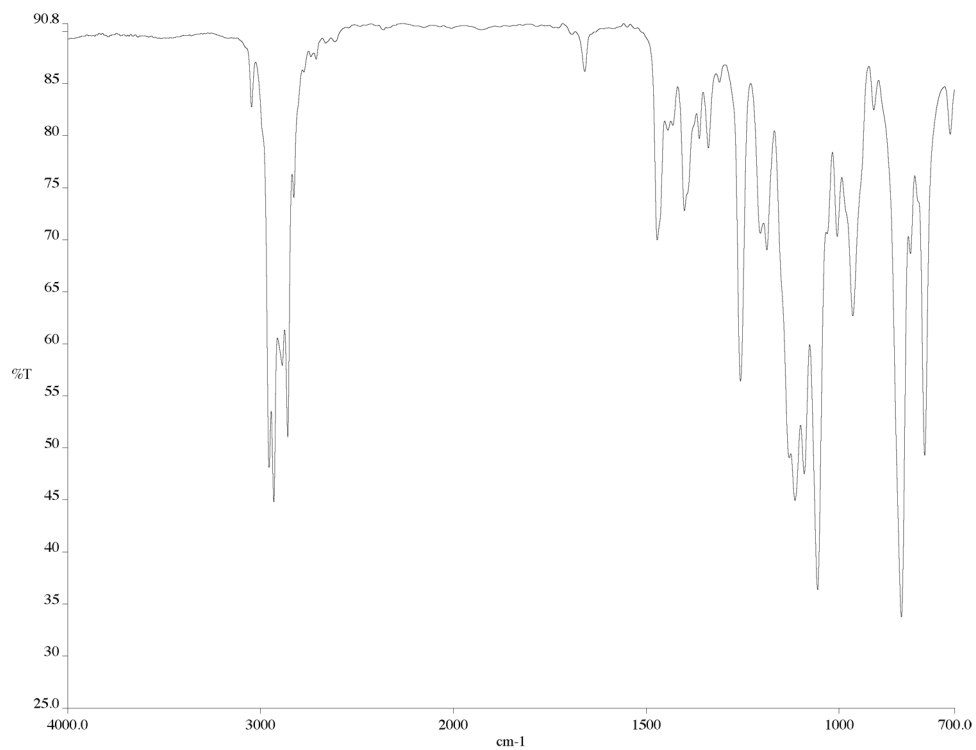


Figure A1.2 Infrared spectrum (thin film/NaCl) of compound **63**.

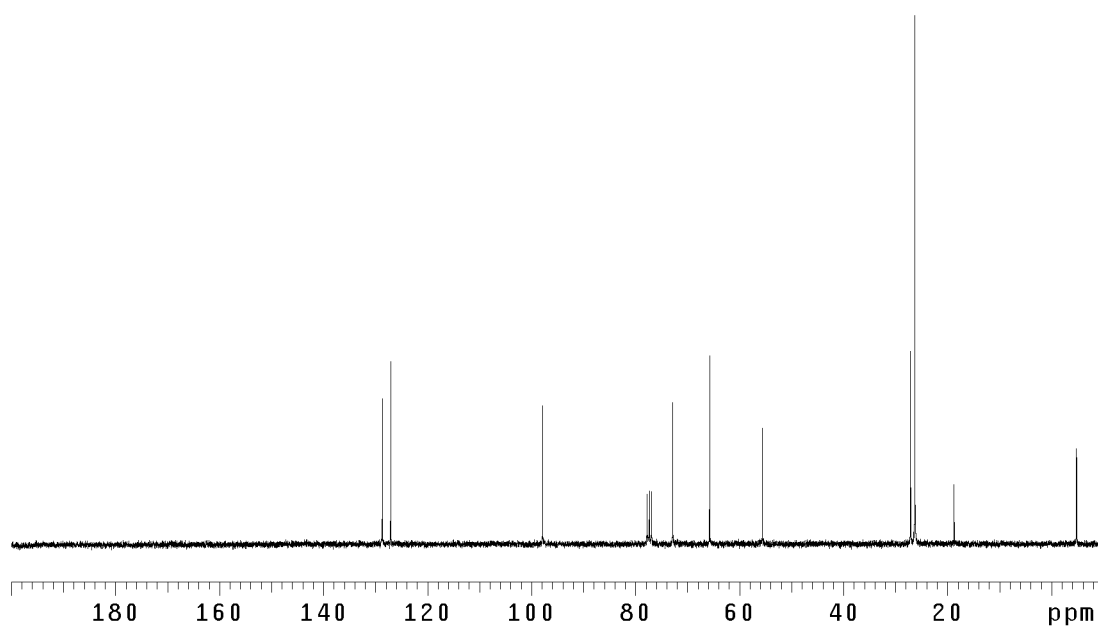


Figure A1.3 ^{13}C NMR (125 MHz, CDCl_3) of compound **63**.

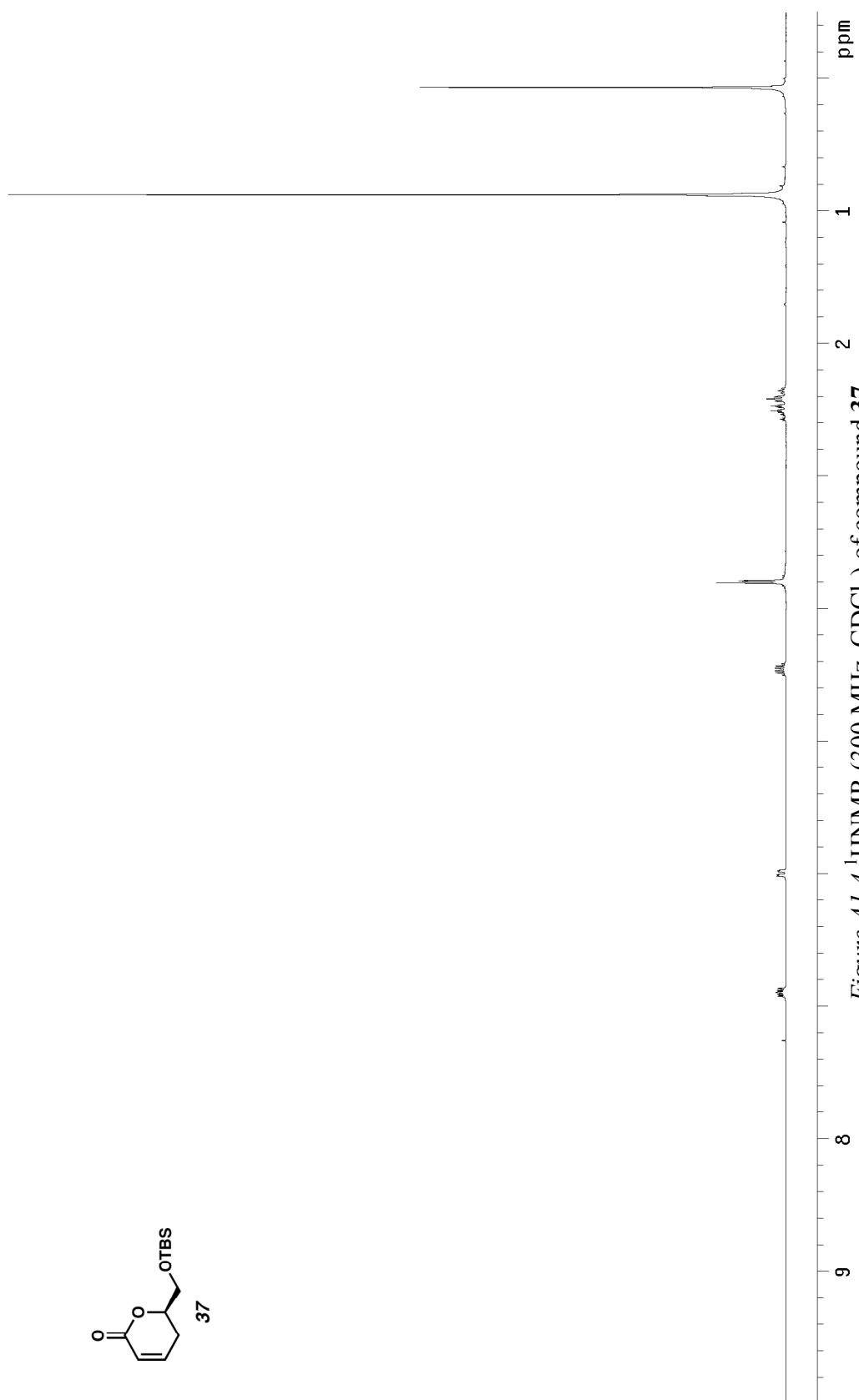
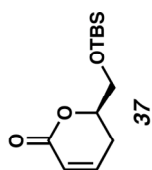


Figure A1.4 ¹H NMR (300 MHz, CDCl₃) of compound 37.

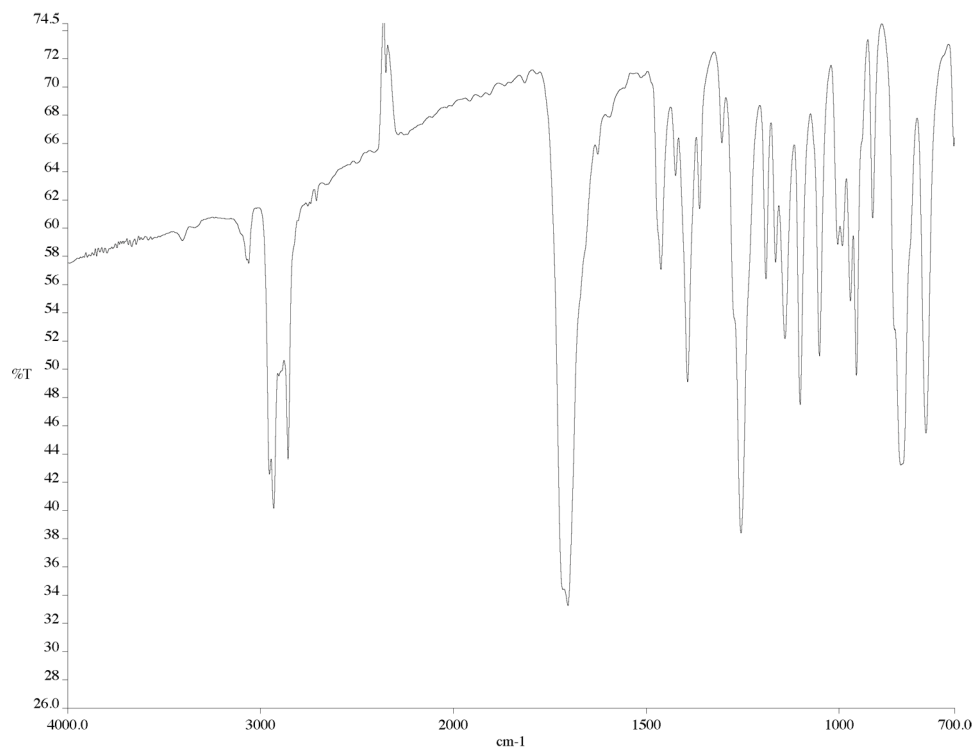


Figure A1.5 Infrared spectrum (thin film/NaCl) of compound 37.

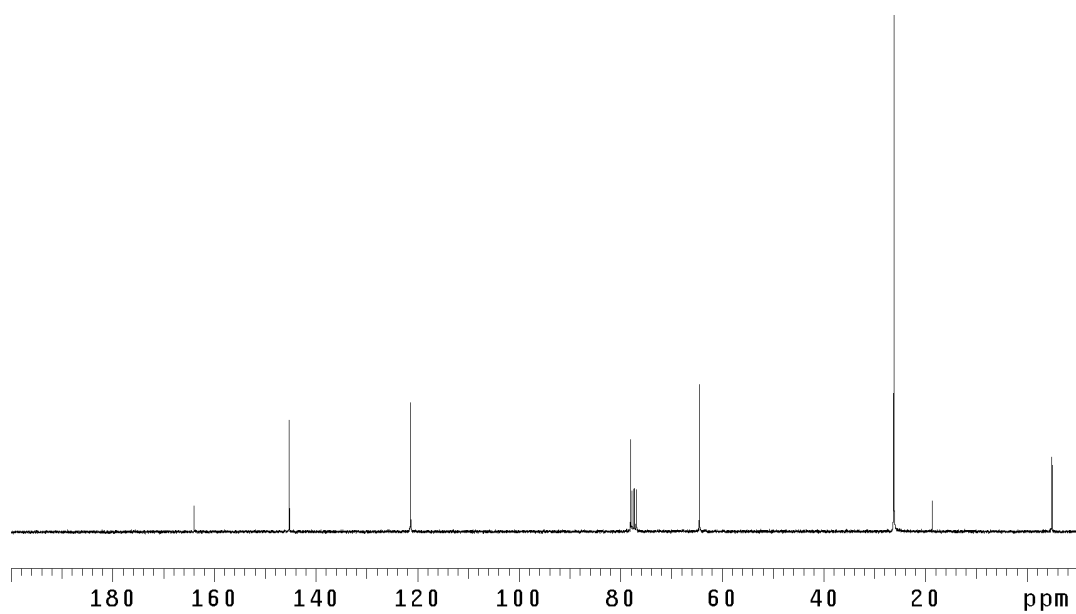


Figure A1.6 ¹³C NMR (125 MHz, CDCl₃) of compound 37.

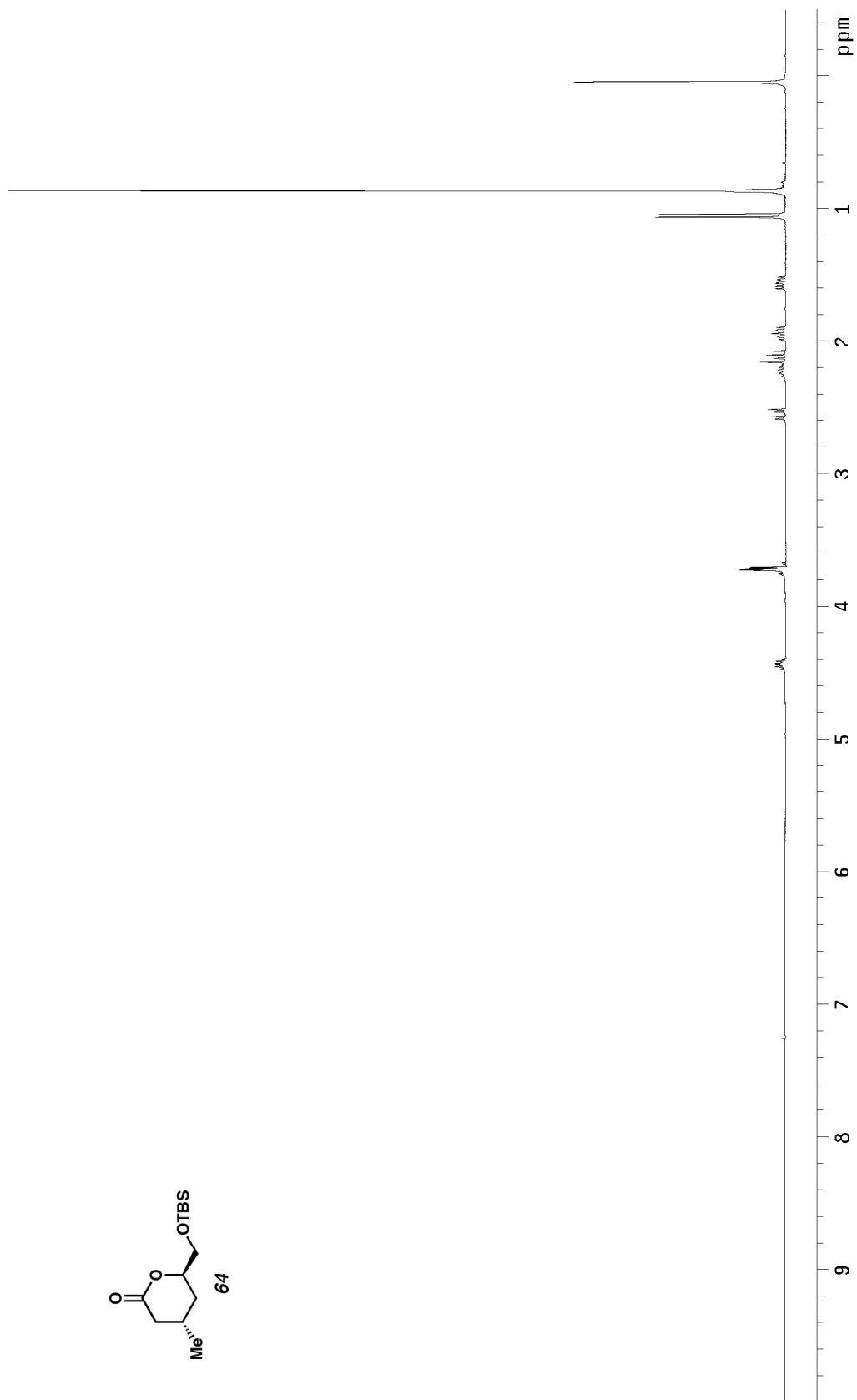
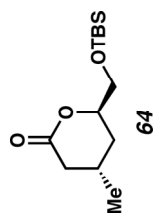


Figure A1.7 $^1\text{H NMR}$ (300 MHz, CDCl_3) of compound **64**.

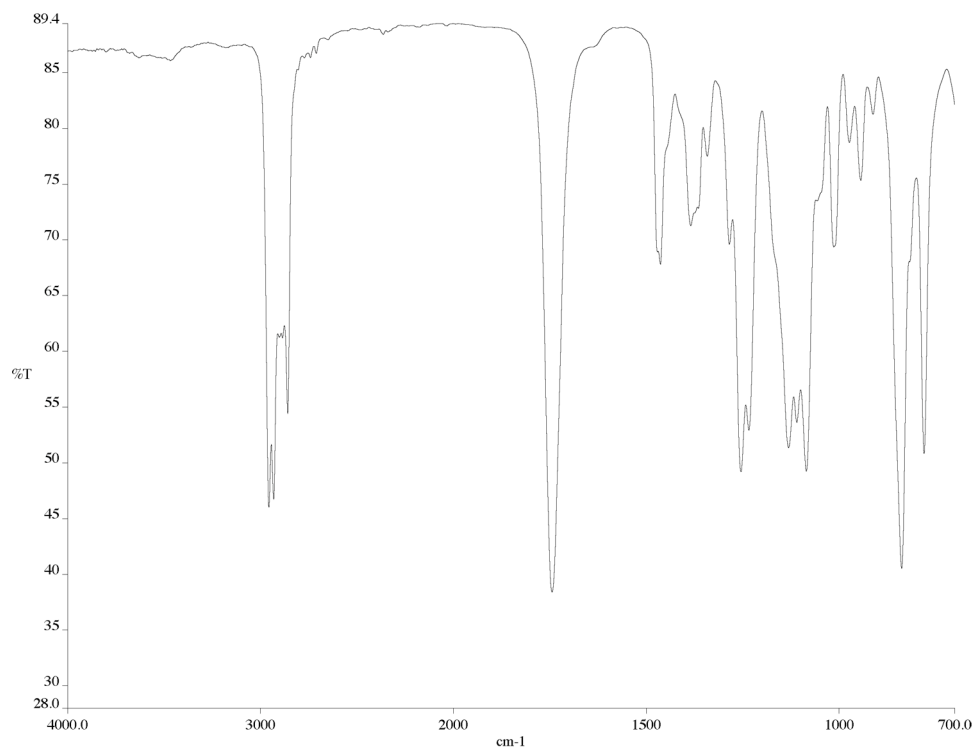


Figure A1.8 Infrared spectrum (thin film/NaCl) of compound **64**.

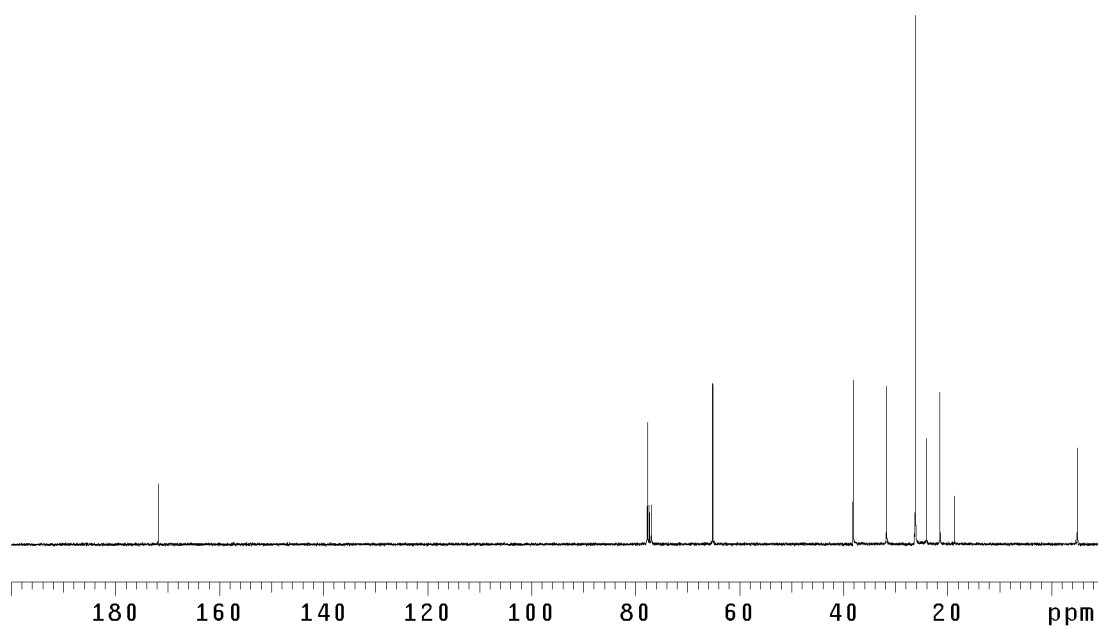


Figure A1.9 ¹³C NMR (125 MHz, CDCl₃) of compound **64**.

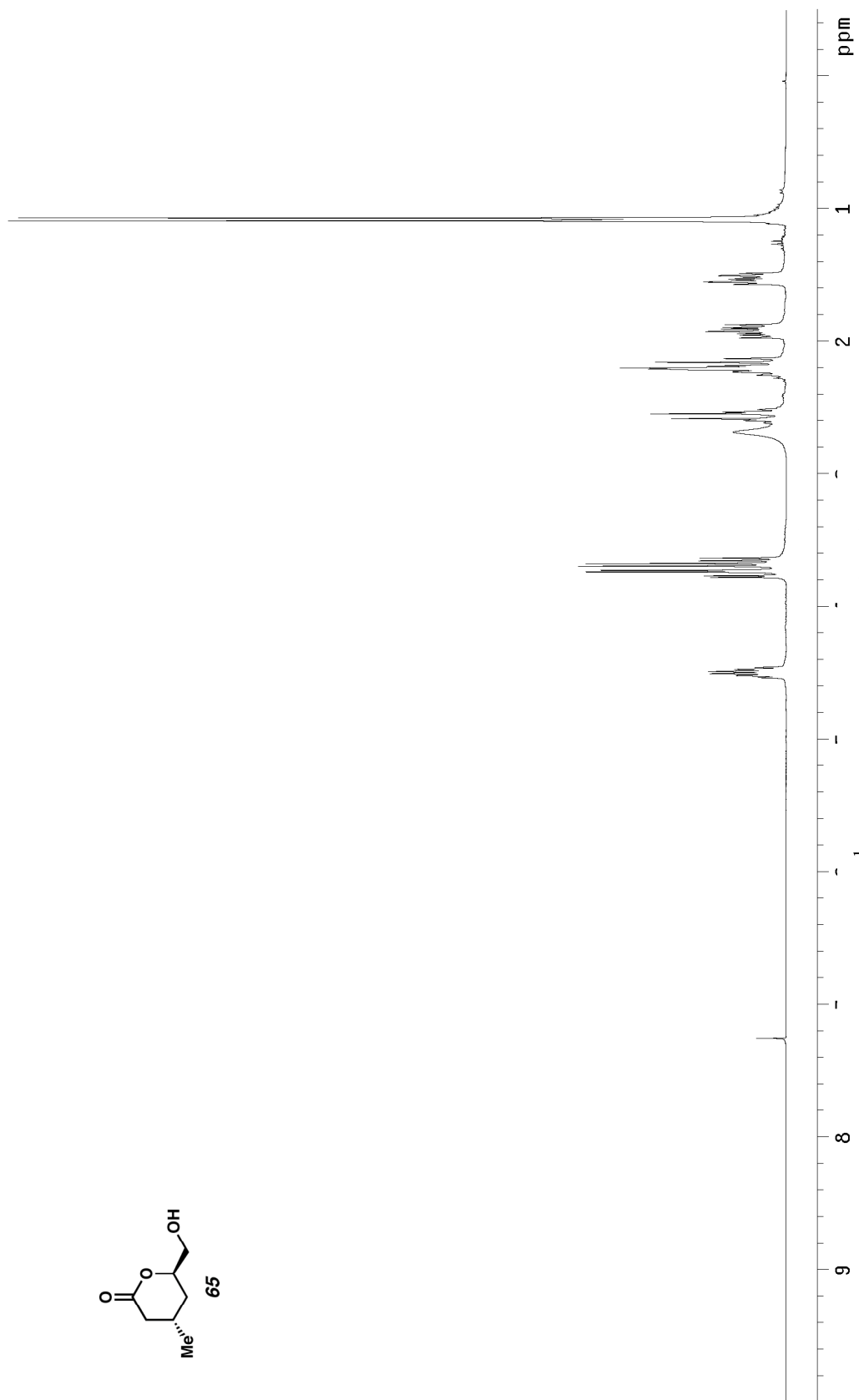
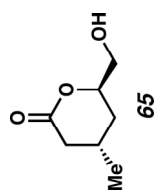


Figure A1.10 $^1\text{H NMR}$ (300 MHz, CDCl_3) of compound **65**.

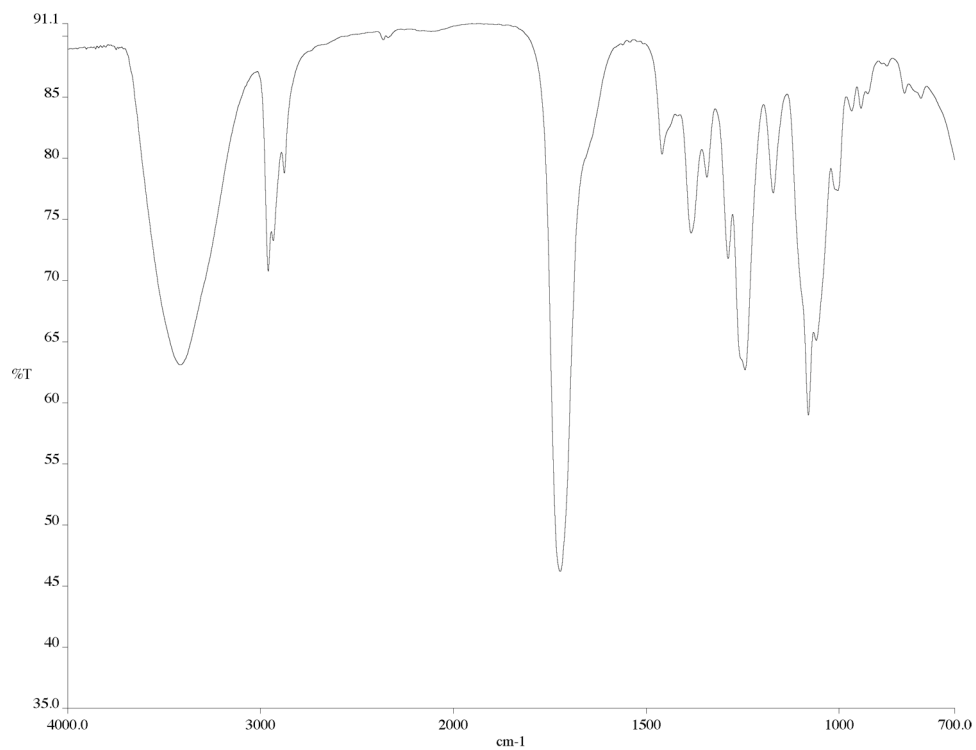


Figure A1.11 Infrared spectrum (thin film/NaCl) of compound **65**.

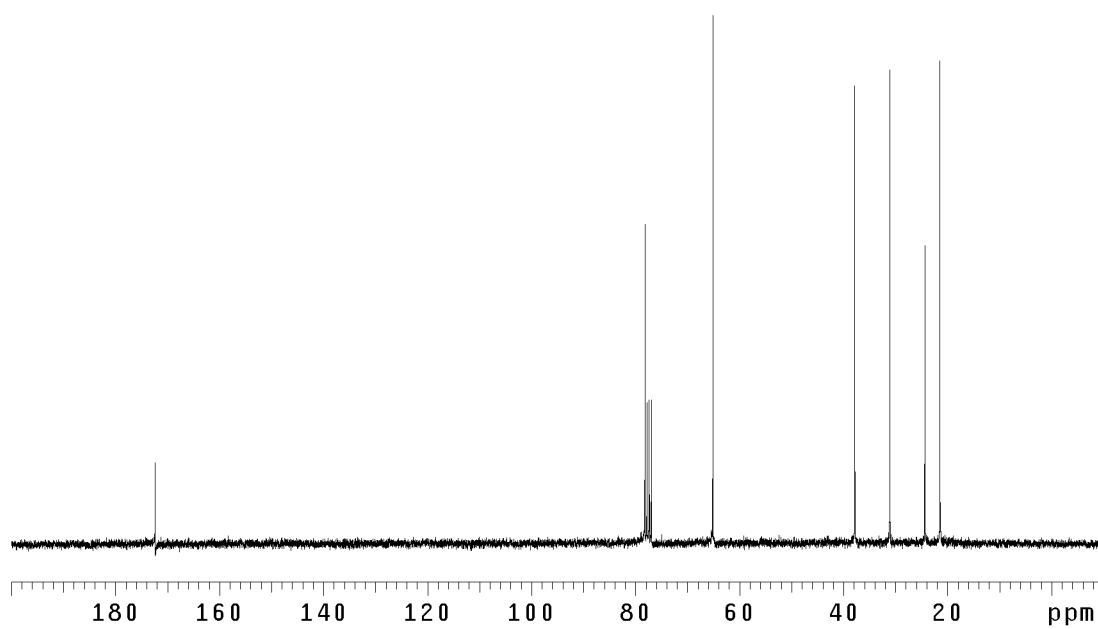


Figure A1.12 ¹³CNMR (125 MHz, CDCl₃) of compound **65**.

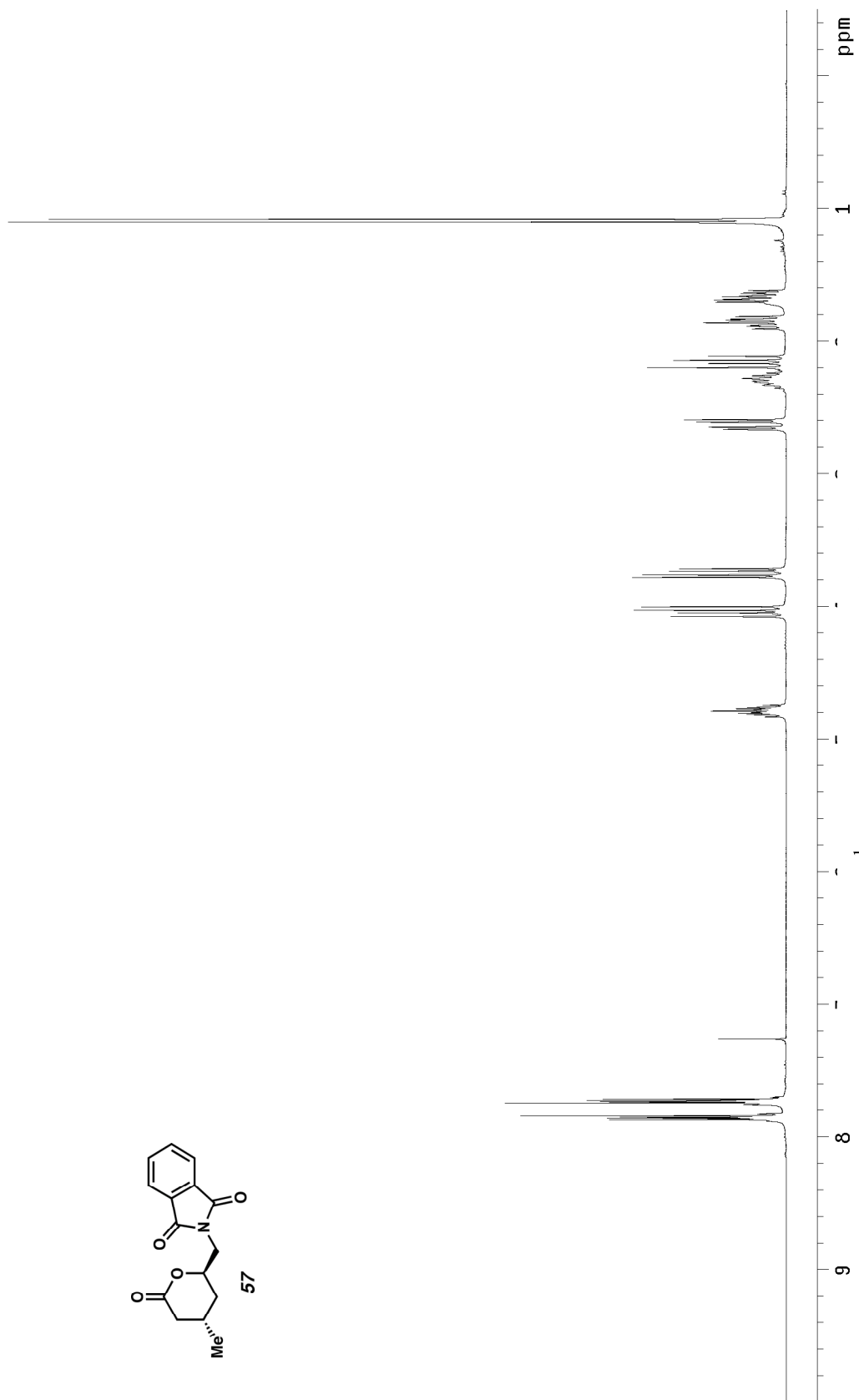
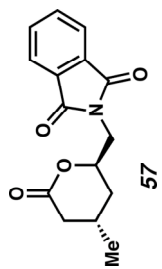


Figure A1.13 $^1\text{H NMR}$ (300 MHz, CDCl_3) of compound **57**.

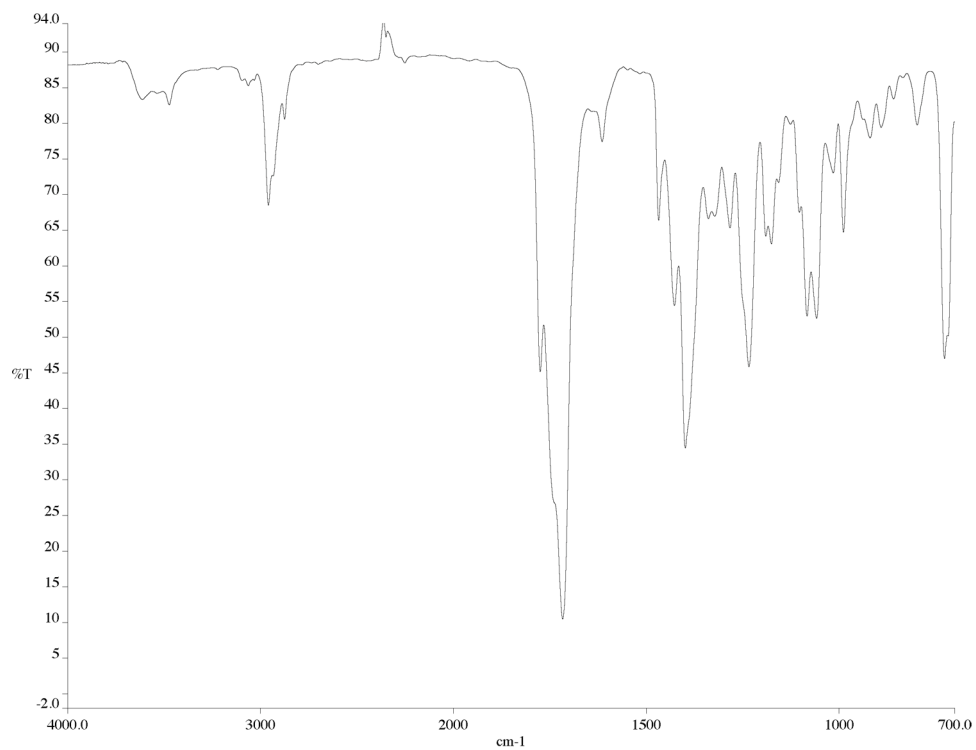


Figure A1.14 Infrared spectrum (thin film/NaCl) of compound **57**.

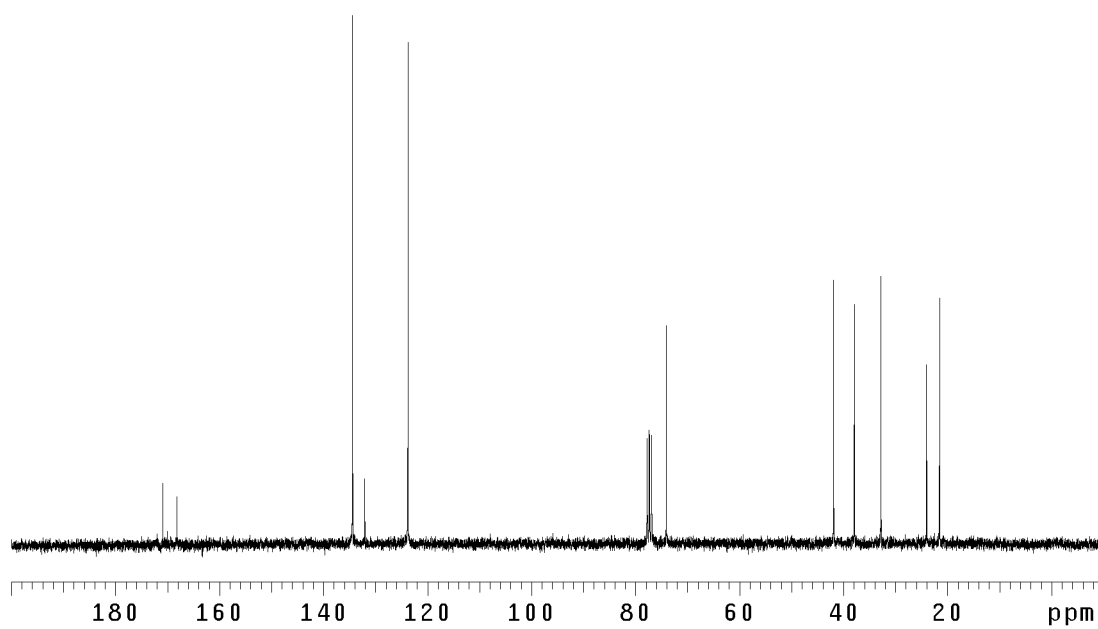


Figure A1.15 ¹³C NMR (125 MHz, CDCl₃) of compound **57**.

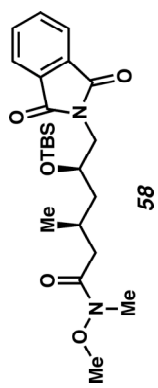
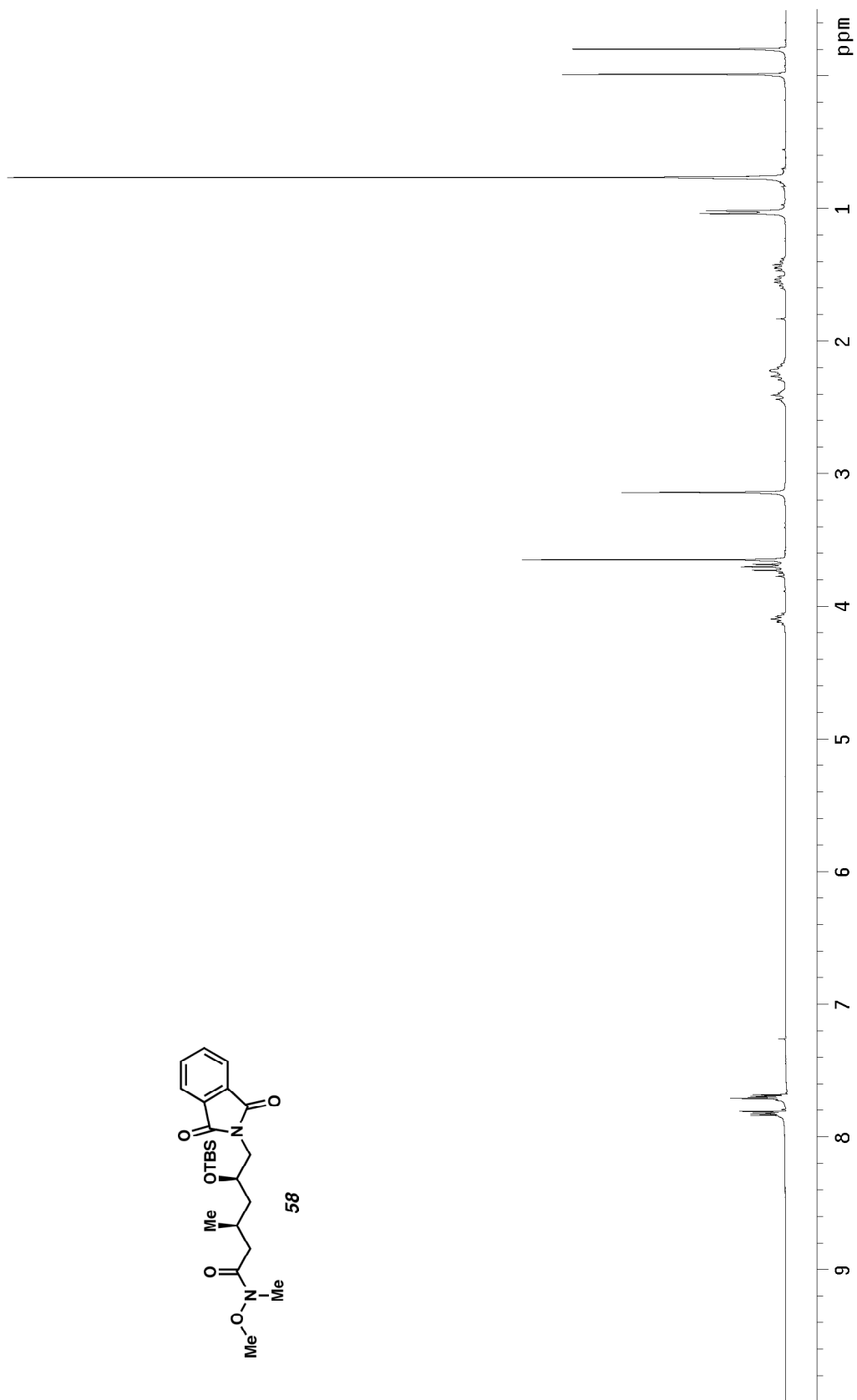


Figure A1.16 ^1H NMR (300 MHz, CDCl_3) of compound **58**.

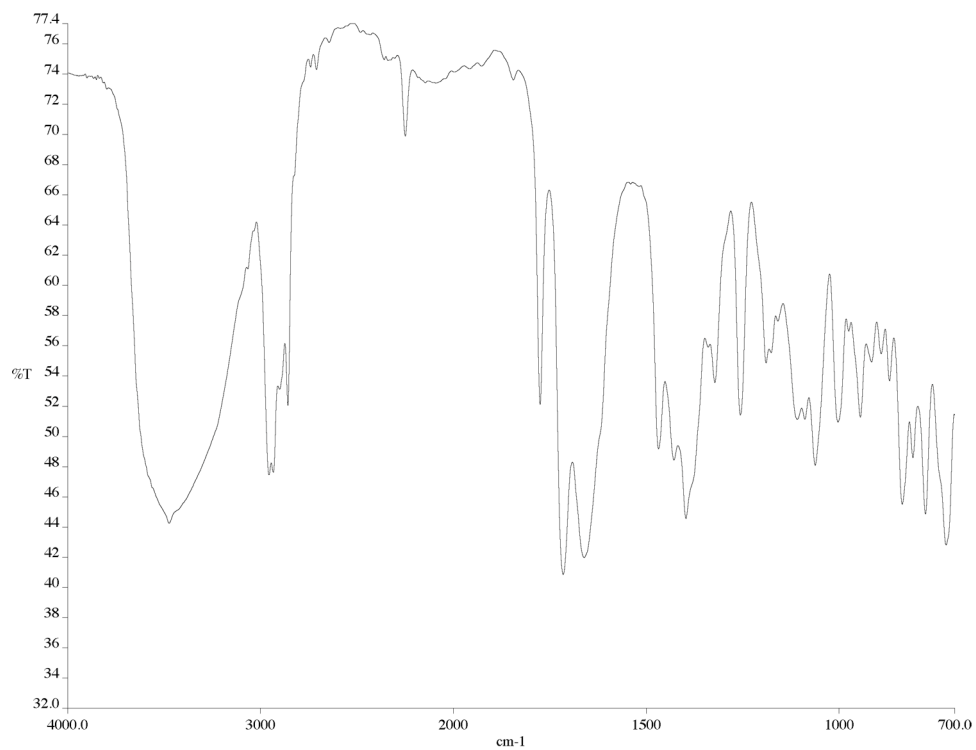


Figure A1.17 Infrared spectrum (thin film/NaCl) of compound **58**.

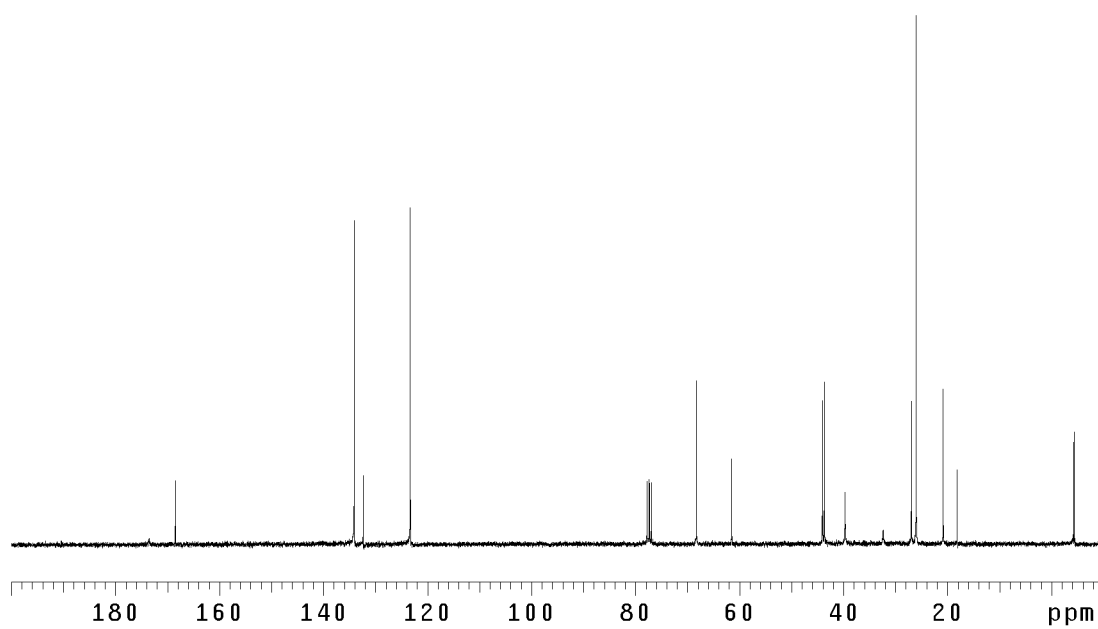


Figure A1.18 ^{13}C NMR (125 MHz, CDCl_3) of compound **58**.

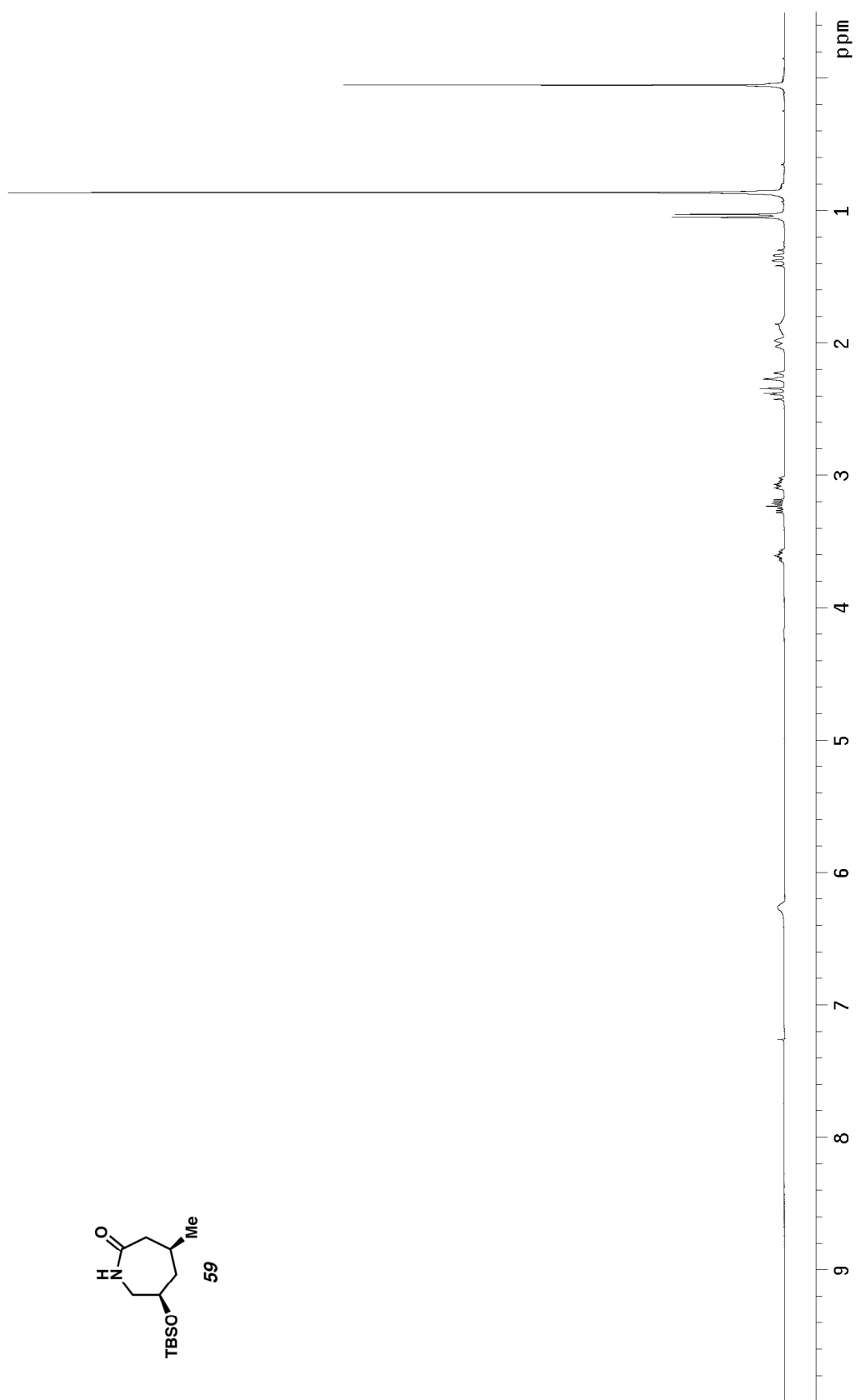


Figure A1.19 ^1H NMR (300 MHz, CDCl_3) of compound **59**.

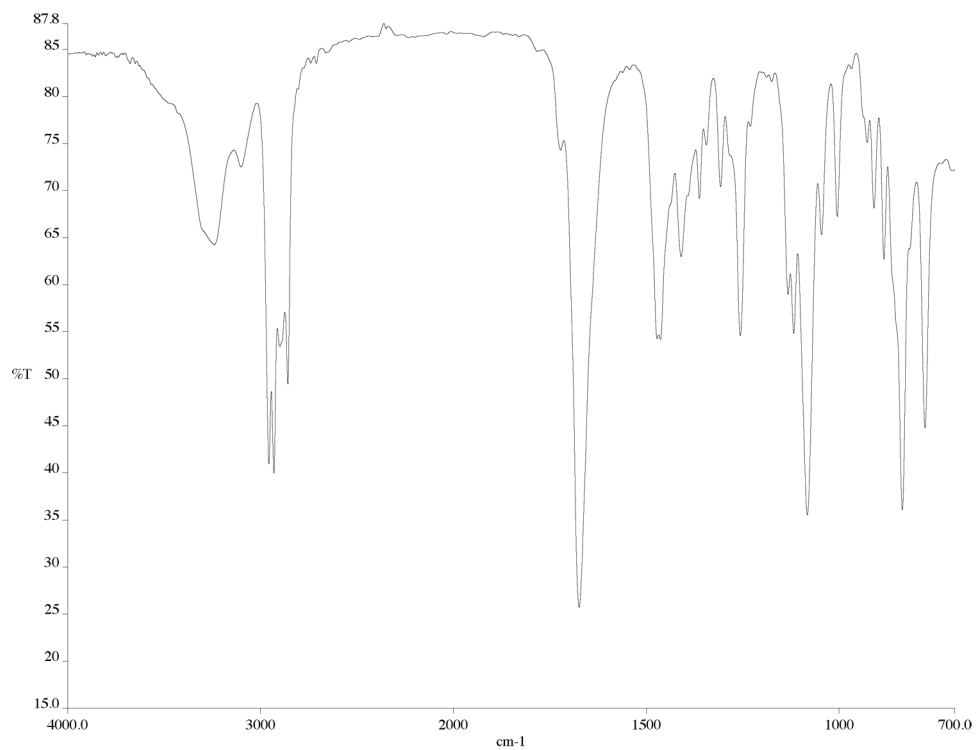


Figure A1.20 Infrared spectrum (thin film/NaCl) of compound **59**.

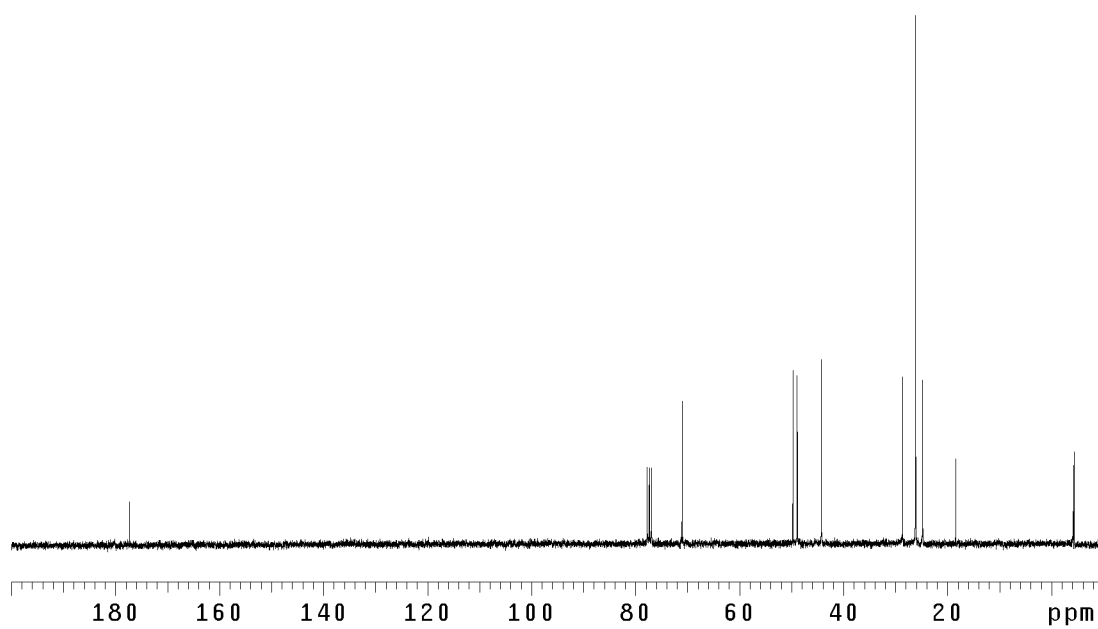


Figure A1.21 ¹³C NMR (125 MHz, CDCl₃) of compound **59**.

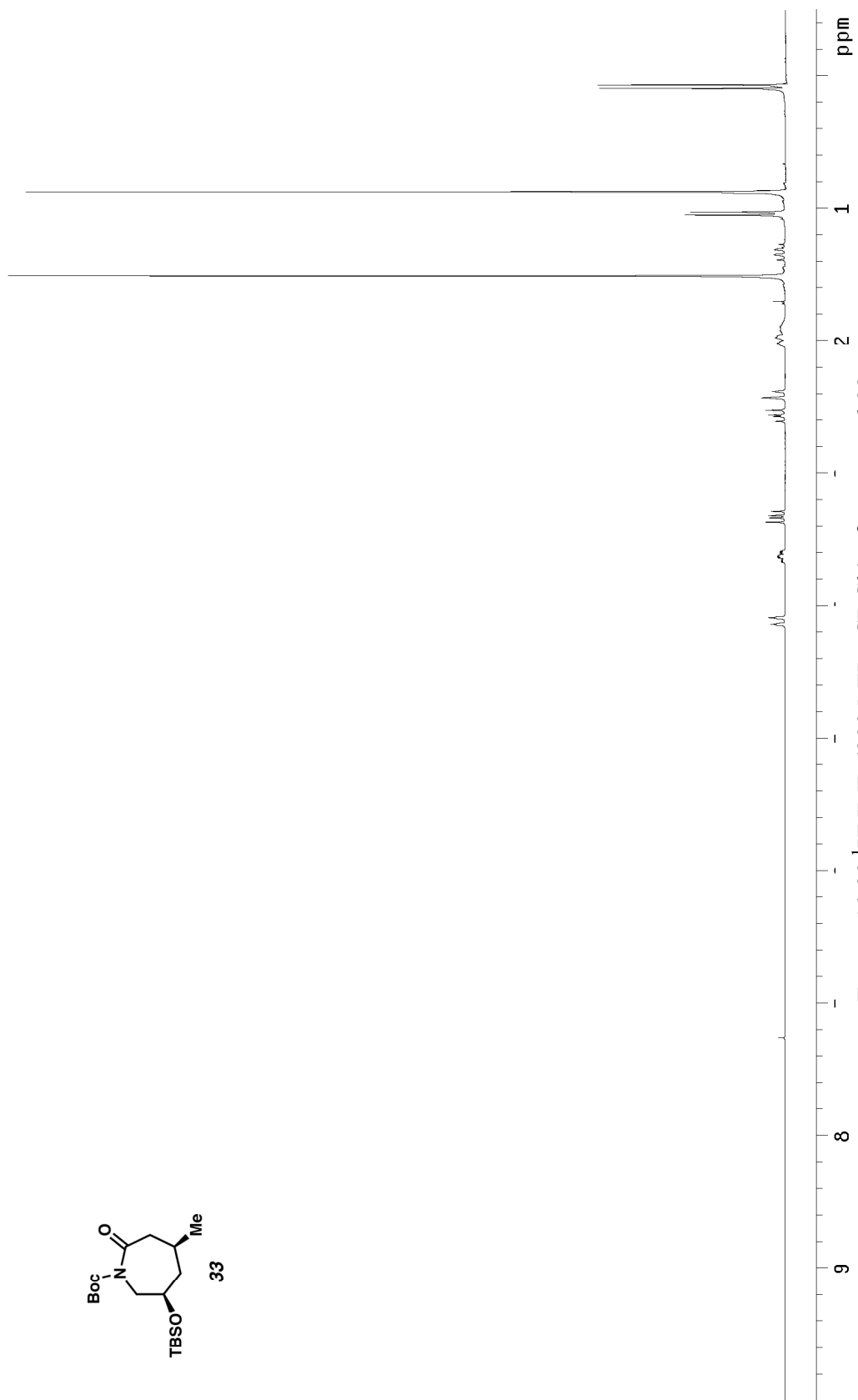
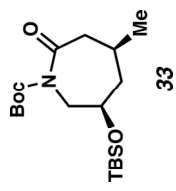


Figure A1.22 ¹H NMR (300 MHz, CDCl₃) of compound 33.

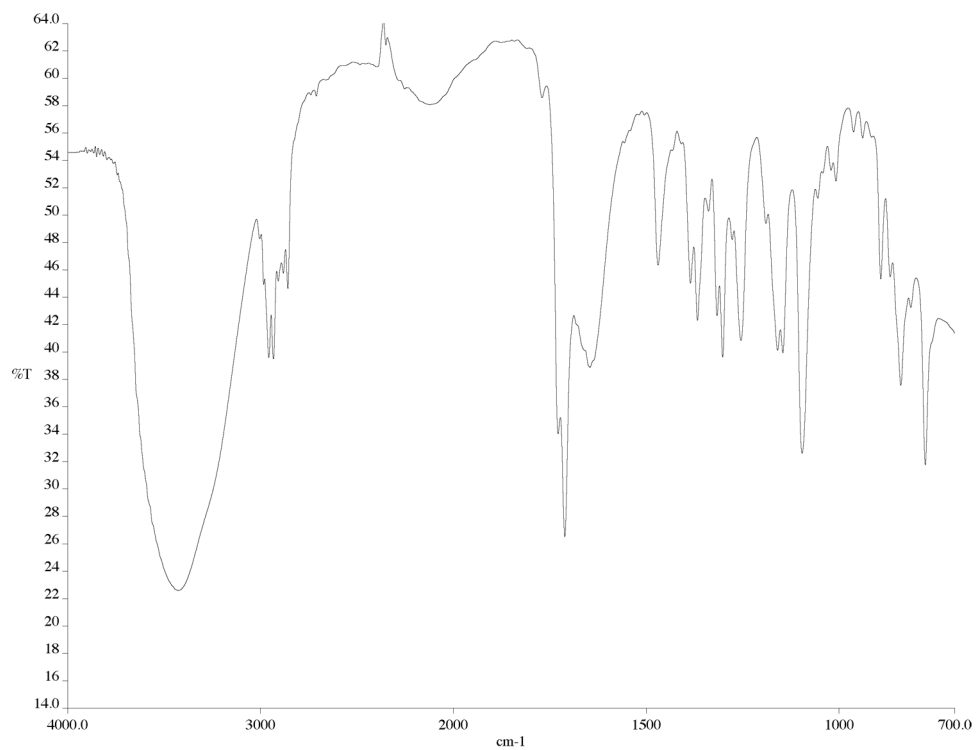


Figure A1.23 Infrared spectrum (thin film/NaCl) of compound **33**.

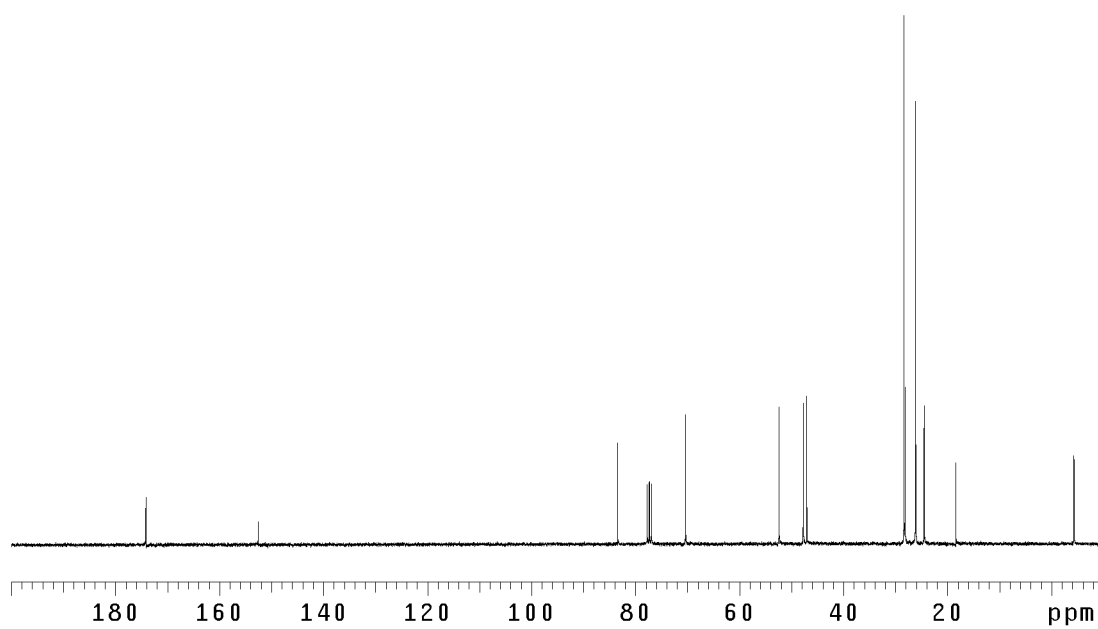
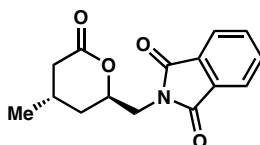


Figure A1.24 ¹³CNMR (125 MHz, CDCl₃) of compound **33**.

X-Ray Crystallographic Data

2-(((2*R*,4*S*)-4-methyl-6-oxotetrahydro-2*H*-pyran-2-yl)
methyl)isoindoline-1,3-dione



Contents

Table 1.	Crystal data
Figures	Figures for publication
Table 2.	Atomic coordinates
Table 3.	Selected bond distances and angles
Table 4.	Full bond distances and angles (for deposit)
Table 5.	Anisotropic displacement parameters

Table 1. Crystal data and structure refinement for JTB01 (CCDC 181862).

Empirical formula	C ₁₅ H ₁₅ NO ₄
Formula weight	273.28
Crystallization solvent	Heptane/ethylacetate
Crystal habit	Tabular
Crystal size	0.53 x 0.30 x 0.24 mm ³
Crystal color	Colorless

Data Collection

Preliminary Photos	Rotation	
Type of diffractometer	Bruker P4	
Wavelength	0.71073 Å MoK α	
Data Collection Temperature	98(2) K	
θ range for 7982 reflections used in lattice determination	2.33 to 27.55°	
Unit cell dimensions	a = 7.0241(7) Å b = 19.2892(19) Å c = 10.3911(10) Å	β = 109.578(2)°
Volume	1326.5(2) Å ³	
Z	4	
Crystal system	Monoclinic	
Space group	P2 ₁ /n	
Density (calculated)	1.368 Mg/m ³	
F(000)	576	
Data collection program	Bruker SMART v5.054	
θ range for data collection	2.11 to 27.89°	
Completeness to θ = 27.89°	94.1 %	
Index ranges	-9 ≤ h ≤ 8, -25 ≤ k ≤ 25, -13 ≤ l ≤ 13	
Data collection scan type	ω scans at 5 ϕ settings	
Data reduction program	Bruker SAINT v6.022	
Reflections collected	18272	
Independent reflections	2992 [R _{int} = 0.0434]	
Absorption coefficient	0.100 mm ⁻¹	
Absorption correction	None	
Max. and min. transmission	0.9764 and 0.9489	

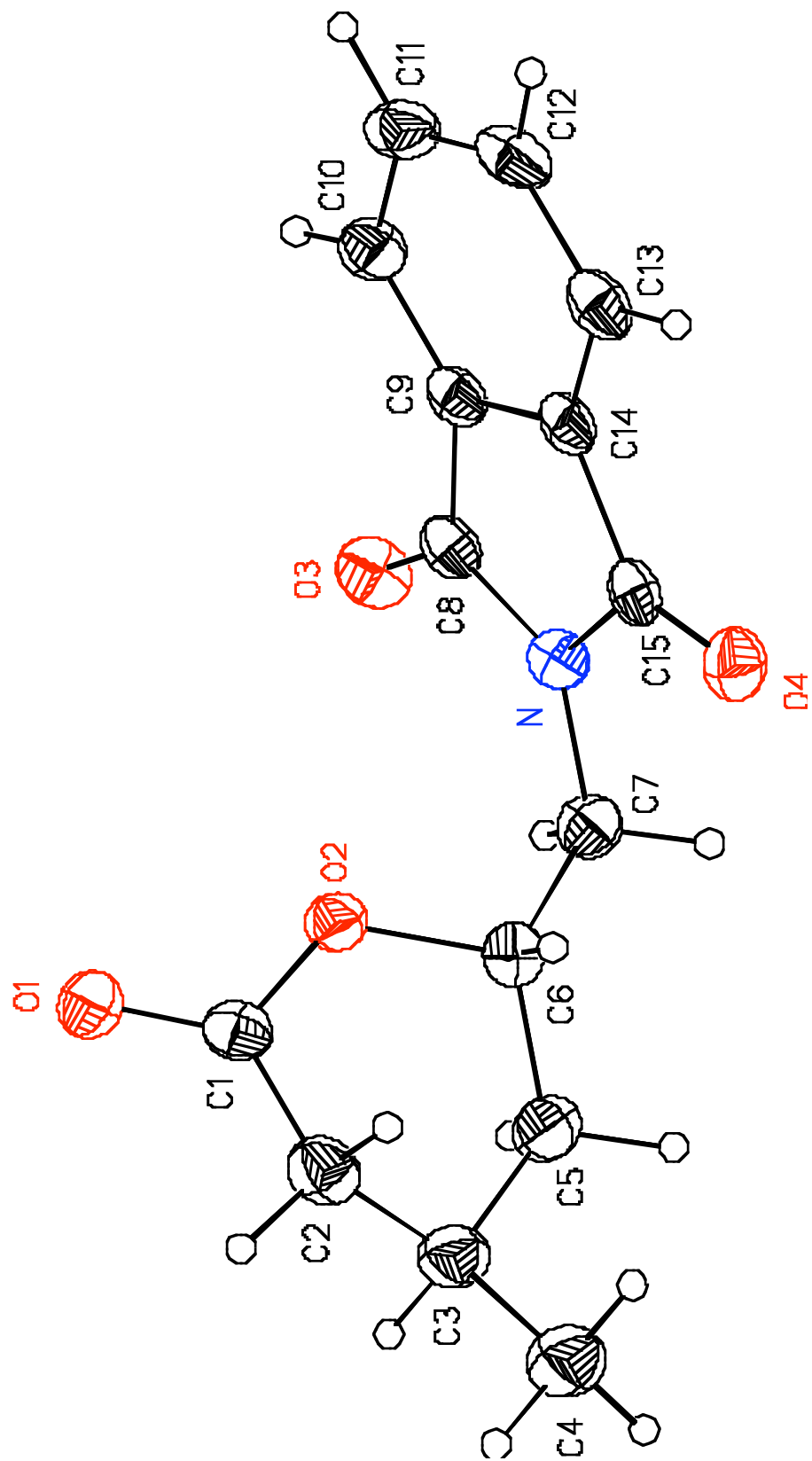
Table 1 (cont.)**Structure Solution and Refinement**

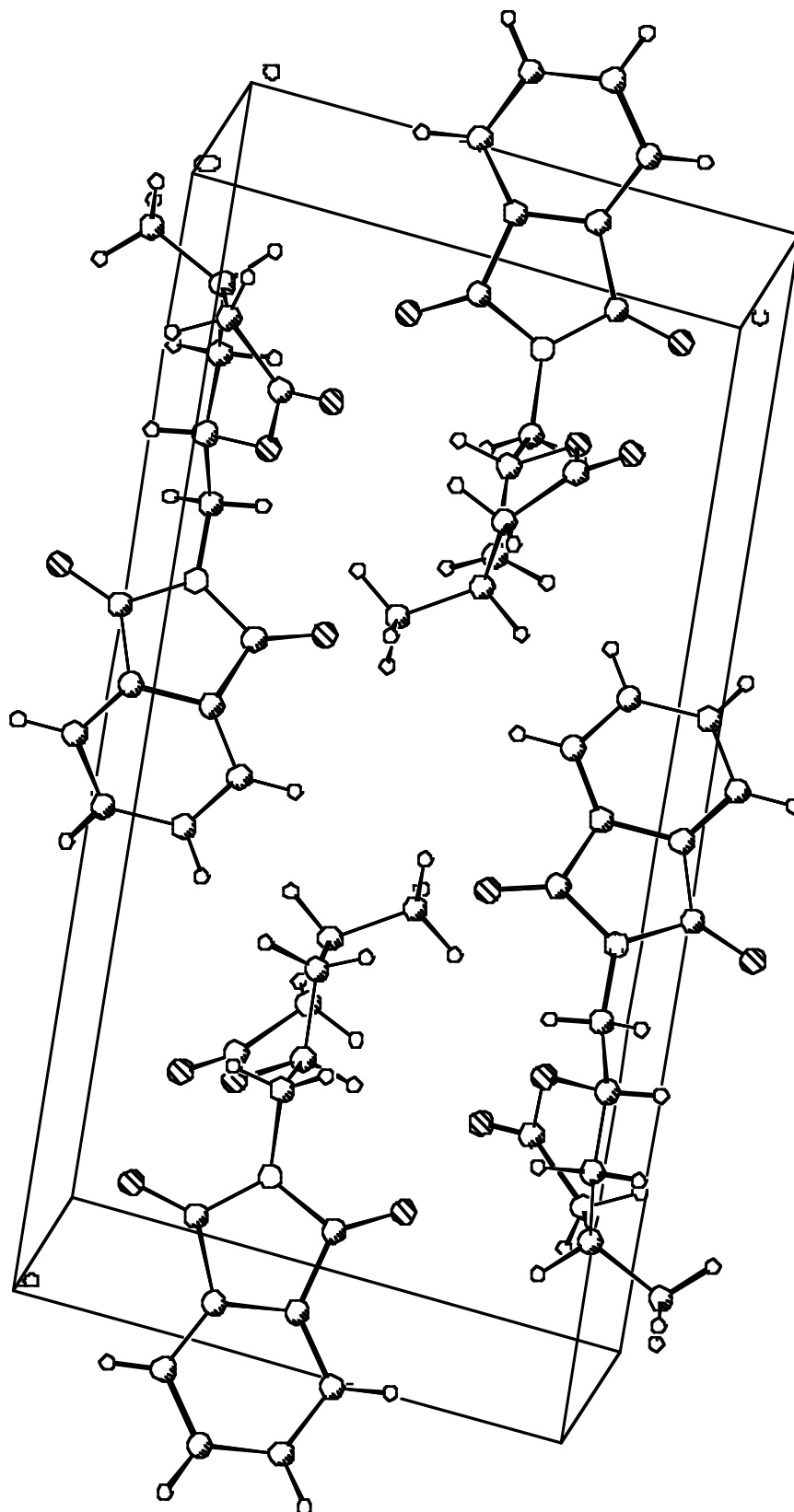
Structure solution program	SHELXS-97 (Sheldrick, 1990)
Primary solution method	Direct methods
Secondary solution method	Difference Fourier map
Hydrogen placement	Difference Fourier map
Structure refinement program	SHELXL-97 (Sheldrick, 1997)
Refinement method	Full matrix least-squares on F^2
Data / restraints / parameters	2992 / 0 / 241
Treatment of hydrogen atoms	Unrestrained
Goodness-of-fit on F^2	2.274
Final R indices [$I > 2\sigma(I)$, 2323 reflections]	$R1 = 0.0428$, $wR2 = 0.0682$
R indices (all data)	$R1 = 0.0579$, $wR2 = 0.0692$
Type of weighting scheme used	Sigma
Weighting scheme used	$w=1/\sigma^2(F_o^2)$
Max shift/error	0.000
Average shift/error	0.000
Largest diff. peak and hole	0.298 and -0.245 e. \AA^{-3}

Special Refinement Details

Refinement of F^2 against ALL reflections. The weighted R-factor (wR) and goodness of fit (S) are based on F^2 , conventional R-factors (R) are based on F , with F set to zero for negative F^2 . The threshold expression of $F^2 > 2s(F^2)$ is used only for calculating R-factors(gt) etc. and is not relevant to the choice of reflections for refinement. R-factors based on F^2 are statistically about twice as large as those based on F , and R-factors based on ALL data will be even larger.

All esds (except the esd in the dihedral angle between two l.s. planes) are estimated using the full covariance matrix. The cell esds are taken into account individually in the estimation of esds in distances, angles and torsion angles; correlations between esds in cell parameters are only used when they are defined by crystal symmetry. An approximate (isotropic) treatment of cell esds is used for estimating esds involving l.s. planes.





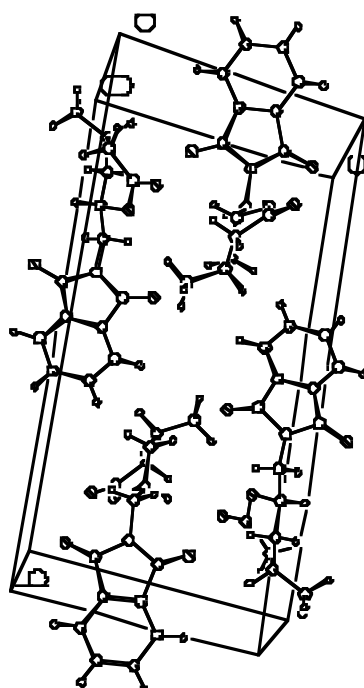
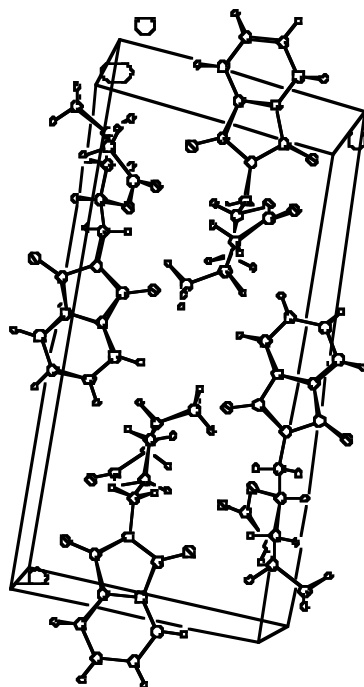


Table 2. Atomic coordinates ($\times 10^4$) and equivalent isotropic displacement parameters ($\text{\AA}^2 \times 10^3$) for JTB01 (CCDC 181862). $U(\text{eq})$ is defined as the trace of the orthogonalized U^{ij} tensor.

	x	y	z	U_{eq}
O(1)	8436(1)	2407(1)	2404(1)	32(1)
O(2)	5191(1)	2656(1)	1692(1)	27(1)
O(3)	3360(1)	3947(1)	3345(1)	33(1)
O(4)	1021(1)	3763(1)	-1307(1)	33(1)
N	2145(2)	3677(1)	1039(1)	24(1)
C(1)	6761(2)	2271(1)	1623(1)	26(1)
C(2)	6257(2)	1726(1)	544(2)	34(1)
C(3)	4416(2)	1280(1)	485(2)	34(1)
C(4)	3661(3)	892(1)	-851(2)	43(1)
C(5)	2781(2)	1731(1)	758(2)	32(1)
C(6)	3201(2)	2493(1)	708(2)	27(1)
C(7)	1738(2)	2943(1)	1113(2)	28(1)
C(8)	2953(2)	4115(1)	2163(1)	25(1)
C(9)	3146(2)	4805(1)	1580(1)	24(1)
C(10)	3904(2)	5421(1)	2214(2)	30(1)
C(11)	3914(2)	5986(1)	1383(2)	34(1)
C(12)	3170(2)	5931(1)	-26(2)	32(1)
C(13)	2400(2)	5310(1)	-662(2)	29(1)
C(14)	2416(2)	4750(1)	168(1)	23(1)
C(15)	1753(2)	4027(1)	-194(1)	24(1)

Table 3. Bond lengths [Å] and angles [°] for JTB01 (CCDC 181862).

O(1)-C(1)	1.2131(16)	C(4)-C(3)-C(5)	113.28(14)
O(2)-C(1)	1.3515(15)	C(2)-C(3)-C(5)	110.22(12)
O(2)-C(6)	1.4634(16)	C(4)-C(3)-H(3)	108.4(7)
O(3)-C(8)	1.2081(14)	C(2)-C(3)-H(3)	106.2(7)
O(4)-C(15)	1.2093(15)	C(5)-C(3)-H(3)	108.2(7)
N-C(15)	1.3913(16)	C(3)-C(4)-H(4A)	110.1(8)
N-C(8)	1.3973(16)	C(3)-C(4)-H(4B)	107.8(7)
N-C(7)	1.4525(17)	H(4A)-C(4)-H(4B)	108.8(11)
C(1)-C(2)	1.4899(19)	C(3)-C(4)-H(4C)	108.8(9)
C(2)-C(3)	1.537(2)	H(4A)-C(4)-H(4C)	109.4(12)
C(2)-H(2A)	0.976(14)	H(4B)-C(4)-H(4C)	111.9(12)
C(2)-H(2B)	0.995(14)	C(6)-C(5)-C(3)	112.23(12)
C(3)-C(4)	1.509(2)	C(6)-C(5)-H(5A)	107.5(8)
C(3)-C(5)	1.541(2)	C(3)-C(5)-H(5A)	111.4(7)
C(3)-H(3)	1.036(13)	C(6)-C(5)-H(5B)	106.7(7)
C(4)-H(4A)	1.057(16)	C(3)-C(5)-H(5B)	111.0(7)
C(4)-H(4B)	1.060(14)	H(5A)-C(5)-H(5B)	107.7(11)
C(4)-H(4C)	1.026(17)	O(2)-C(6)-C(5)	109.82(11)
C(5)-C(6)	1.5024(19)	O(2)-C(6)-C(7)	105.13(11)
C(5)-H(5A)	1.037(15)	C(5)-C(6)-C(7)	113.12(12)
C(5)-H(5B)	1.052(13)	O(2)-C(6)-H(6)	108.5(7)
C(6)-C(7)	1.5088(19)	C(5)-C(6)-H(6)	106.2(7)
C(6)-H(6)	1.018(12)	C(7)-C(6)-H(6)	114.0(7)
C(7)-H(7A)	0.943(13)	N-C(7)-C(6)	112.46(11)
C(7)-H(7B)	0.984(13)	N-C(7)-H(7A)	107.1(8)
C(8)-C(9)	1.4882(18)	C(6)-C(7)-H(7A)	110.3(8)
C(9)-C(10)	1.3757(19)	N-C(7)-H(7B)	108.1(7)
C(9)-C(14)	1.3866(18)	C(6)-C(7)-H(7B)	109.0(7)
C(10)-C(11)	1.391(2)	H(7A)-C(7)-H(7B)	109.9(11)
C(10)-H(10)	0.952(13)	O(3)-C(8)-N	125.45(12)
C(11)-C(12)	1.384(2)	O(3)-C(8)-C(9)	129.04(13)
C(11)-H(11)	0.959(13)	N-C(8)-C(9)	105.50(11)
C(12)-C(13)	1.387(2)	C(10)-C(9)-C(14)	121.29(13)
C(12)-H(12)	0.960(13)	C(10)-C(9)-C(8)	130.66(13)
C(13)-C(14)	1.3795(18)	C(14)-C(9)-C(8)	108.04(12)
C(13)-H(13)	0.975(12)	C(9)-C(10)-C(11)	117.42(14)
C(14)-C(15)	1.4788(18)	C(9)-C(10)-H(10)	121.0(8)
C(1)-O(2)-C(6)	116.71(10)	C(11)-C(10)-H(10)	121.5(8)
C(15)-N-C(8)	112.13(11)	C(12)-C(11)-C(10)	121.18(15)
C(15)-N-C(7)	122.64(12)	C(12)-C(11)-H(11)	119.5(8)
C(8)-N-C(7)	125.22(11)	C(10)-C(11)-H(11)	119.4(8)
O(1)-C(1)-O(2)	118.14(12)	C(11)-C(12)-C(13)	121.26(14)
O(1)-C(1)-C(2)	126.02(13)	C(11)-C(12)-H(12)	119.4(8)
O(2)-C(1)-C(2)	115.82(13)	C(13)-C(12)-H(12)	119.3(8)
C(1)-C(2)-C(3)	114.18(12)	C(14)-C(13)-C(12)	117.24(14)
C(1)-C(2)-H(2A)	108.5(8)	C(14)-C(13)-H(13)	121.7(7)
C(3)-C(2)-H(2A)	111.5(8)	C(12)-C(13)-H(13)	121.0(7)
C(1)-C(2)-H(2B)	108.7(8)	C(13)-C(14)-C(9)	121.60(13)
C(3)-C(2)-H(2B)	104.4(9)	C(13)-C(14)-C(15)	130.02(13)
H(2A)-C(2)-H(2B)	109.3(11)	C(9)-C(14)-C(15)	108.37(12)
C(4)-C(3)-C(2)	110.27(13)	O(4)-C(15)-N	124.54(12)

O(4)-C(15)-C(14)

129.54(13)

N-C(15)-C(14)

105.92(11)

Table 4. Anisotropic displacement parameters ($\text{\AA}^2 \times 10^4$) for JTB01 (CCDC 181862). The anisotropic displacement factor exponent takes the form: $-2\pi^2 [h^2 a^{*2} U^{11} + \dots + 2 h k a^* b^* U^{12}]$

	U^{11}	U^{22}	U^{33}	U^{23}	U^{13}	U^{12}
O(1)	274(6)	301(6)	372(6)	0(5)	108(5)	-30(5)
O(2)	247(5)	231(5)	327(6)	-18(4)	110(5)	-13(4)
O(3)	397(6)	350(6)	256(6)	42(5)	142(5)	51(5)
O(4)	305(6)	376(6)	264(6)	-5(5)	49(5)	1(5)
N	238(6)	239(6)	253(6)	23(5)	105(5)	11(5)
C(1)	314(9)	227(8)	272(8)	59(6)	135(7)	3(7)
C(2)	357(10)	350(9)	318(9)	-33(7)	139(8)	68(7)
C(3)	407(10)	279(8)	295(9)	-32(7)	87(7)	23(7)
C(4)	496(12)	372(10)	376(11)	-71(8)	92(9)	19(9)
C(5)	340(10)	286(9)	315(9)	-21(7)	91(8)	-36(7)
C(6)	257(8)	290(8)	271(8)	0(7)	81(7)	0(6)
C(7)	275(9)	268(8)	313(9)	22(7)	120(7)	-29(7)
C(8)	217(8)	285(8)	267(8)	21(6)	118(6)	56(6)
C(9)	194(7)	256(8)	293(8)	29(6)	121(6)	52(6)
C(10)	280(8)	285(8)	355(9)	-38(7)	136(7)	40(7)
C(11)	293(9)	245(8)	537(11)	-35(8)	210(8)	13(7)
C(12)	290(9)	260(8)	493(11)	125(8)	225(8)	79(7)
C(13)	235(8)	337(9)	319(9)	85(7)	141(7)	69(7)
C(14)	158(7)	270(8)	295(8)	34(6)	107(6)	49(6)
C(15)	157(7)	307(8)	266(8)	30(7)	79(6)	36(6)

Table 5. Hydrogen coordinates ($\times 10^4$) and isotropic displacement parameters ($\text{\AA}^2 \times 10^3$) for JTB01 (CCDC 181862).

	x	y	z	U_{iso}
H(2A)	7460(20)	1442(7)	672(13)	36(4)
H(2B)	5870(20)	1955(8)	-365(15)	46(5)
H(3)	4920(20)	922(7)	1269(13)	38(4)
H(4A)	4850(20)	602(8)	-998(14)	54(5)
H(4B)	2520(20)	546(7)	-800(13)	41(4)
H(4C)	3130(20)	1243(9)	-1632(16)	64(5)
H(5A)	1360(20)	1636(7)	47(14)	42(4)
H(5B)	2700(20)	1631(7)	1732(14)	37(4)
H(6)	3229(18)	2588(6)	-250(13)	22(3)
H(7A)	1826(19)	2848(6)	2021(14)	29(4)
H(7B)	360(20)	2850(6)	493(13)	27(4)
H(10)	4410(20)	5457(6)	3184(14)	29(4)
H(11)	4470(20)	6418(7)	1795(13)	31(4)
H(12)	3220(20)	6327(7)	-574(13)	33(4)
H(13)	1905(18)	5270(6)	-1655(13)	24(4)